2022

# Using Drones to Evaluate Revegetation Success on Natural Gas Pipelines

Anthony Nelson Mesa
*West Virginia University*, anm0041@mix.wvu.edu

# Using Drones to Evaluate Revegetation Success on Natural Gas Pipelines

**Anthony N. Mesa**

**Thesis submitted**
**to the Davis College of Agriculture, Natural Resources and Design**
**at West Virginia University**

**in partial fulfillment of the requirements for the degree of**

**The Master of Science in**
**Energy Environments**

**Shawn Grushecky, Ph.D., Chair**
**Paul Kinder, Ph.D.**
**Michael Strager, Ph.D.**

**Department of Energy Environments**

**Morgantown, West Virginia**
**2022**

**Keywords:** Pipeline, Multispectral, UAV, Revegetation, SVM

## Abstract

Using drones to evaluate revegetation success on natural gas pipelines

Anthony N. Mesa

The Appalachian region of the United States has significant growth in the production of natural gas. Developing the infrastructure required for this resource creates significant disturbances across the landscape, as both well pads and transportation pipelines must be created in this mountainous terrain. Midstream infrastructure, which includes pipeline rights-of-way and associated infrastructure, can cause significant environmental degradation, especially in the form of sedimentation. The introduction of this non-point source pollutant can be detrimental to freshwater ecosystems found throughout this region. This ecological risk has necessitated the enactment of regulations related to midstream infrastructure development. Weekly, inspectors travel afoot along pipeline rights-of-way, monitoring the reestablishment of surface vegetation and identifying failing areas for future management. The topographically challenging terrain of West Virginia makes these inspections difficult and dangerous to the hiking inspectors. We evaluated the accuracy at which unmanned aerial vehicles replicated inspector classifications to evaluate their use as a complementary tool in the pipeline inspection process. Both RGB and multispectral sensor collections were performed, and a support vector machine classification model predicting vegetation cover were made for each dataset. Using inspector defined validation plots, our research found comparable high accuracy between the two collection sensors. This technique appears to be capable of augmenting the current inspection process, though it is likely that the model can be improved to help lower overall costs. The high accuracy thus obtained suggests valuable implementation of this widely available technology in aiding these challenging inspections.

## Acknowledgements

Special acknowledgement to Sam Bearinger and Lucas Kinder of the WVU Natural Resource Analysis Center who helped to fly and process the UAV imagery. This project was supported by funding from the United States Department of Transportation Pipeline and Hazardous Materials Safety Administration. And lastly, this work was also supported by the USDA National Institute of Food and Agriculture, Hatch project accession number 1015648, and the West Virginia Agricultural and Forestry Experiment Station.

## Table of Contents

## List of Tables

## List of Figures

## Introduction

When considering the application of modern techniques into traditional practices, modernity must undergo an evaluation of its capabilities at replicating the task at hand. Gains in efficiency and safety must have their accuracy and precision costs weighed. Unmanned aerial vehicles (UAVs or drones), remotely piloted aircraft capable of varied data collection and often equipped with visual sensors (Alley-Young, 2020), have found such measures to be in their favor internationally. Many industries have witnessed their inclusion to effect new functionality or augment and enhance existing techniques. Industrial facilities with dangerous or inaccessible structures in need of safety inspections have been able to include UAVs in their operations to minimize risk without sacrificing evaluation coverage (Nikolic et al., 2013). Civil engineers needing to inspect large structures for minor faults have found the value in UAV inclusion (Hallermann and Morgenthal, 2014). Agricultural operations utilize UAVs equipped with multispectral sensors to optimize fertilizer application and harvest (Kim et al., 2019). With the realized value found in so many diverse sectors of industry, the performance potential in novel utilization is worthy of calculating.

Natural gas (NG) production in the United States (US) has surpassed that of all other countries (Doman and Kahan, 2018). Of the natural gas development regions in the US, the Appalachian basin has been developed into the largest NG producer, producing 33% of the total national output (U.S. Department of Energy, 2020; U.S. Energy Information Administration, 2021). NG is rich in this region due to two shale plays extending beneath it. They are known as the Marcellus and Utica shales, which extend across 298,000 $km^2$ and 240,000 $km^2$ respectively (Kargbo et al., 2010; Popova, 2017a; Popova, 2017b). Modern unconventional drilling and

hydraulic fracturing (fracking) techniques have led to the large growth seen in this region, which is projected to double its NG productivity by 2050 (U.S. Department of Energy, 2020).

Typical NG production in the Appalachian basin begins with the establishment of a well pad, whereupon unconventional wells are established. These wells draw from a large area of the NG bearing shale with vertical well bore descending up to 2.4 km in depth with a lateral leg that can extend over 6 km (Marcellus Drilling News, 2021). NG flowing to the surface from this process is directed into a near surface gathering pipeline (midstream), through which it travels to the fuel's final users. The midstream is lined with compressor stations to maintain the pipeline's pressure (Messersmith et al., 2015). Each midstream compressor station is situated upon its own pad structure. In all, the installation of the pad and midstream infrastructure require large quantities of land alterations, potentially causing large ecological disturbance events across the landscape, with midstream segments creating the greatest footprint of landscape impact (Langlois et al., 2017).

In the early stages of development, standing timber and surface vegetation are removed, and the land surface is graded across the extent of the NG infrastructure. Development of NG resources has been found to significantly impact surface water flow (Warner et al., 2013) and total suspended solids (TSS) quantities in associated watersheds (Olmstead et al., 2013). Further, increased sediment in freshwater ecosystems has caused significant ecologic impacts. Sediment introduction has been found to decrease the populations of lower trophic level aquatic species (Richards and Bacon, 1994), and lead to severe reduction in primary producers' photosynthetic activity and overall health (Cederholm and Lestelle, 1974). At higher trophic levels, larger vertebrates show organ damage and recruitment loss in sediment rich waterways (Kemp et al., 2011).

The potential for such drastic ecological impacts has prompted the regulation of NG from both state and federal agencies across the US. Federally, the US Environmental Protection Agency, Clean Water Act (CWA) Section 404, prohibits companies from discharging sediments and establishes a specific permitting process for NG development. In the Appalachian basin state of West Virginia (WV), the Department of Environmental Protection (DEP) provides development advice as well as regulates NG development within their borders. Advice comes in the form of a best management practice manual (West Virginia Department of Environmental Protection, 2016), which notes the establishment of surface vegetation as the most important act in sediment and erosion control on NG sites. This importance is codified in the General Water Pollution Control Permit (GWPCP) agreed to by NG development companies (West Virginia Department of Environmental Protection, 2013). This permit directs the inspection and vegetation standards necessary for a company's bond to be released.

Frequent site inspections are to be conducted by a permitee, both weekly and after a significant rain event of over 0.25 in (0.635 cm). Inspections are conducted by certified site inspectors, who travel the whole pipeline length on-foot. Typically, permitees divide the pipeline into inspection sections. Under the GWPCP sediment reduction adherence, hiking inspectors look for vegetation failures, surface soil movement, or failure of erosion control structures of a site. Finding any failure requires immediate reporting, and the issue to be addressed promptly. When a permitee believes a site to be stable, the WV DEP provides their own afoot inspectors to evaluate the site. State inspectors evaluate the permanence of erosion control measures, as well as the health and quantity of surface vegetation on all permeable surfaces. When a site passes this inspection, it is declared to have reached final stabilization, and the bond is returned to the permitee.

As outlined in the GWPCP, passing vegetation coverage is defined as a minimum of 70% surface vegetation across the site. Current afoot inspections determine this coverage with a surface sampling ring, approximately 0.75 $m^2$ to 1 $m^2$ in area. During the state's inspection, this hoop is randomly cast many times throughout the permit area. Wherever the ring lands, the inspector provides an ocular estimation of the vegetation coverage within. The sampling ring is not mentioned in the GWPCP, and there is no further guidance on evaluating this 70% standard. Frequently, a single random sample from within the site judged to be below 70% will generate a failing report from the state inspector, keeping the permit open, and the weekly inspections ongoing.

UAVs could be used as a supplementary tool in this inspection process. The mountainous terrain of the Appalachian region makes frequent afoot inspections both difficult and an ongoing safety concern for the inspectors. Moreover, remote sensing may provide a more objective approach to vegetation evaluations. Though UAVs have addressed the needs and safety concerns of many industries, to the best of our knowledge, the use of UAVs in inspecting NG pipeline vegetation coverage has not yet been evaluated for either accuracy or financial viability. Our research sought to provide insight into both of these aspects. The initial assessment of the accuracy provided by drones in NG inspections was completed using machine learning classifier models created from two widely available UAV sensor technologies, simple RGB and agriculturally designed multispectral capture. The evaluation of these technologies will provide an introductory evaluation of the accuracy gap between current standards and novel techniques. Financial evaluations were derived from the recorded research efforts and compared to self-reported performance standards provided by individuals active in this industry. As the agricultural industry has had notable success in evaluating vegetation with multispectral

collection and analysis, we expect that the multispectral data will accurately identify inspector assessments. Similarly, the technology's financial benefit to the agricultural industry raises the expectation that similar financial benefits will be seen when drones are used in NG pipeline inspections.

## Methods

### Study Area

An industry partner provided access to a recently completed pipeline in northern West Virginia for the execution of this project. This area was comprised of two branches of a continuous pipeline separated by a natural gas well pad (Figure 1). The combined length of the two branches was approximately 2.3 km, and when impervious surfaces were excluded, approximately 6.2 ha of managed and monitored pipeline was available for analysis. The southern branch was approved for release several years ago and is bordered by forested lands. The northern branch completed construction and installation in early 2021 and runs through lands used for livestock grazing. There is no physical barrier barring animals from grazing upon the pipeline area. The elevation in the study area ranges from about 326 m – 414 m MSL, with greatest slopes being around 57%. Flow interruption angled water bars are created along all pipeline areas with significant length and slope. Additional erosion control features on the test site include the surface application of hay, coir mats, hydro-seed, silt socks, and silt fences.

### Test Plots and Classification

The study area's permit holder allowed the establishment of 30 small unobtrusive testing plots for the purpose of conducting a vegetation analysis. A field technician from the West

Virginia University (WVU) Natural Resources Analysis Center (NRAC) was equipped with a Garmin Dakota 10 and tasked with creating these plots. Across the study area, 30 randomly placed plots were established (Figure 2). Each plot was created using high-visibility survey marking spray to create the 4 corners surrounding an area of approximately 1.44 $m^2$ (1.2 m × 1.2 m) (Figure 3). This size was selected to allow the internal area of each plot to provide an area of approximately 1 $m^2$ of pixels unaltered by the survey marking spray. This area was selected after interviewing several pipeline inspectors, as a sample size of 1 $m^2$ was stated as the size used for current evaluations as captured from a randomly cast surface sampling hoop. To create continuity between foot and drone imagery, the top of each test plot was indicated by a solid line connecting the two respective corners, and a two-digit number was created just outside and beneath the bottom right corner. Numbers ranged from 00 – 29. Upon completion of marking the plot, an image was captured using a hand-held 12-megapixel camera from a height of approximately 1.8 m. These ground perspective high-resolution images were collected for the future integration of subject matter expert (SME) classification into this study.

After establishing a sample plot, the field technician recorded the approximate center in the handheld GPS unit and indicated whether they assessed the plot to be passing or failing. These categories were defined from current inspection practices, as laid out by the WVDEP (West Virginia Department of Environmental Protection, 2013), passing sites were those where greater than 70% of the internal plot area was vegetated, while failing sites contained less than 70% vegetation. To avoid over-selection from a single area, the field technician was tasked with creating no more than two test plots of the same category within 25 m of each other. This distance was calculated in the field from measurements provided by the handheld GPS unit. Plots

were established in this way across the study area, with 17 plots established in the new branch, and 13 plots in the old branch.

Multispectral Collection

Once sample plots were established, a DJI Matrice 200v2 quad-propeller drone with a direct interfacing Sentera 6x Multispectral sensor conjoined with an apex oriented solar sensor was used for remote data collection. The 6x Multispectral sensor simultaneously collects from 5 individual wavelengths: blue (475 nm), green (550 nm), red (670 nm), red edge (715 nm), and near infrared (NIR, 840 nm). Additionally, the 6x sensor is equipped with a 20MP RGB camera, which provides comparable data capture to the imagery collected by standard drone-based color-image sensors. The Sentera 6x sensor performs a simultaneous capture from all 6 sensors on a preset trigger period. For our collection, we set the trigger to occur every 2 seconds. Flight planning and execution was achieved with the UgCS Client. Through this software we could load in elevation maps, break each branch into transects, and generate a total flight path at a fixed distance above the terrain. The height above terrain used was 91.44 m (300 ft), and the sensor was oriented at nadir throughout the flight. Both flights occurred on the same day between 1130 and 1330 EST to minimize light variance and shadows. Immediately prior to collection, the multispectral sensor captured a series of calibration images of a Sentera Reflectance Panel for future radiometric correction. When the flights were completed, research moved into the analysis portion of the plan of study (Figure 4).

## Plot Classification

Desiring the integration of current inspection quality standards into our study, the research team coordinated with SMEs to collect a classification judgement from each plot. For this area of study, an SME was defined as an individual who had received training and certification in the pipeline inspection process and conducted such inspections in the Appalachian region for a period of at least 5 years. As most approached SMEs were still associated with this industry, anonymity was promised for their assistance.

The previously collected pictures of each plot were shared, and judgments were made as to the official classification of either passing or failing for the plot. Many plots had images taken at different angles with all pictures capturing the same plot being grouped by file. These groups of images were shared on a 17.3 inch 1920 x 1080 monitor in a random order for the classification step. At the request of the inspector, images of any single plot could be switched between, enlarged, and scrolled over to assist in this assessment step. Final classification was determined from the grouped judgment of each plot individually. If the classification was uniform, the plot was classified as either passing or failing as appropriate. If there was a discrepancy in SME classification, we marked the plot as being of an indeterminate class.

## Reflectance Map Creation

The Sentera 6x Multispectral sensor does perform limited on-the-fly sensor adjustments based on changes in detected solar intensity; however, radiometric calibration is only achieved through a post-processing technique provided to the end user by Sentera. This software reviews all collected single band images and detects the calibration images captured pre-flight to determine reflection adjustments to be made. Additionally, the software identifies the sensor

settings and solar readings recorded in the metadata of each image. From these pieces of information, the radiometric correction software adjusts the values of every pixel in the dataset to the reflectance values correct to the atmospheric conditions at collection. The corrected single band images were then loaded into Pix4Dmapper Version 4.6.4 to create total reflectance maps for the site.

Pix4Dmapper aligns the images according to the GPS data recorded in the EXIF portion of each image and begins to identify tie-points between neighboring images. These tie-points guide the final orientation and transformation of each image. The data from the separate bands is also aligned, creating a near absolute georeferencing between the separate simultaneously captured data. The output of this process is a separate single band rasters in the form of an orthomosaic map of the reflectance values, as calculated across the site. This process was repeated with the RGB dataset collected by the 20 MP sensor. 115 ground control points were identified in a composite display of the red, green, and blue reflectance bands, and these points were used to tie the RGB dataset to the reflectance maps. A natural color orthomosaic was then produced and exported for the study area. The spatial resolution of the multispectral raster and the RGB raster were 0.042 m and 0.063 m respectively.

GIS Analysis

The red, green, blue, and NIR reflectance maps, and the RGB orthomosaic for the study area were then loaded into Esri's ArcGIS Pro (Esri, 2021) for preparation, extraction, classification, and analysis. A new set of ground control points, hereafter called the alignment assessment point set (AAPS), were established between the two datasets to quantify any distortion, ensuring the data were reasonably aligned for analysis. Using the RGB orthomosaic of

the site, polygon features were created to approximately digitize the permit areas. All pixels from every dataset within this polygon boundary were extracted for analysis. The single band layers were composited using the Composite Bands tool, and the Band Indices tool was used to calculate a normalized difference vegetation index (NDVI) layer. NDVI acts as a simplified indication of vegetation health by detecting photosynthetic activity (Tucker, 1979). NDVI is calculated for each pixel from collected reflection values of the red and near-infrared (NIR) bands of light as:

$$NDVI = \frac{NIR - Red}{NIR + Red}$$

As solar light reaches a plant, red light is absorbed by the chlorophyll, while the unusable NIR light is reflected or scattered by the mesophyll layer (Campbell and Wynne, 2011). NDVI values range from -1 to 1, with higher scores associated with healthier vegetation and lower scores being associated with artificial objects. Agriculturally minded multispectral sensors, like the Sentera 6x, are often designed for derivative NDVI calculation, and as such, this technique was included. The produced NDVI layer was composited with the clipped single band rasters for simplified inclusion in classification.

Ground sample plots were then digitized using the RGB raster. All 30 plots previously established were successfully identified. The associated plot numbers and determined SME classification were entered for each plot. 1 and 0 was used to indicate passing and failing classification respectively. Plots with an indeterminate classification were left with a null value.

The Training Samples Manager was opened on the multispectral raster. The band combination display of the raster was adjusted to a true color RGB presentation. Using this and

setting the display scale to a fixed 1:100, a GIS technician manually digitized classification training data across the study site. Classes for this training data set were either pass or fail, with the associated values of 1 and 0 respectively. Training samples were to not include any of the digitized ground sample plots and were to be established across various areas of each branch. There were 30 features established each for passing and failing classes in each branch, totaling 120 training features for the study area (Figure 5).

Support Vector Machines (SVM) was the chosen classification algorithm, due to its noted accuracy at smaller spatial resolutions compared to other common algorithms (Sheykhmousa et al., 2020). In ArcGIS Pro, the Train Support Vector Machine Classifier tool was used with both datasets, producing a definition file for each. The maximum number of samples per class was left at the default value of 500 to avoid the over-fit nature of kernel-based classifications (Liu et al., 2017) while avoiding a loss of accuracy from under sampling (Sabat-Tomala et al., 2020). The Classify Raster tool then processed the datasets with their respective SVM definition files, creating sitewide supervised classification of either passing or failing vegetation assessed at the pixel level (Figures 6 and 7).

Replication Accuracy

From the SVM models, the interior of all validation plots were extracted. As passing and failing cells were valued at 1 and 0 respectively, a mean value calculated with the Zonal Statistics as Table tool directly presented a proportion of passing vegetation within each plot. Following the WVDEP definition of passing vegetation (West Virginia Department of Environmental Protection, 2013), mean values above 0.70 were determined to have been modeled as passing, with values below this number indicating a failing plot. A confusion matrix

was then structured for each model, comparing the modeled and SME judgments for these plots, and providing a validation assessment for each model's performance. For each model the user's accuracy, producer's accuracy, overall accuracy, and kappa were calculated.

Financial Analysis

The largest portions of inspection expenditures can be categorized under two groups, equipment costs and labor costs. Equipment costs cover both physical the pieces of equipment and the software necessary to collect, process, and analyze the data. Entries in this category can either be one-time costs, such as drone and sensor, or may have annual costs, like software licenses and equipment insurance. Manpower costs vary by tasking as they are typically calculated hourly, and commonly include an adjustment for overhead to cover the additional costs of having an employee (Weltman, 2019). As inspection costs are realized across variable periods, from hourly to product lifespan, a realized cost standardization was selected of U.S. dollars to kilometer inspected ($/km). This standardization of costs allowed the full realization of all costs associated to an inspection process given a set tasking, as calculated by distance.

UAV financial assessment began during the accuracy assessment portion of this study. As the drone inspection conducted collection and analysis, equipment and software necessary for each step were noted. Additionally, time records were maintained for each step to address the manpower cost portion of analysis. From the larger equipment and software list, entries unique and critical to the UAV method, such as multispectral sensors and GIS analysis software, were selected and used for a final financial analysis. Similarly, the complete time records were reduced to include only those steps which directly contributed to final GIS product used in the accuracy assessment. Current price estimates for equipment, licenses, and services were then

gathered from manufacturers or retailers, as appropriate. Manpower pay rates for GIS collection and processing were determined from expert input and set at $20/hr and $40/hr respectively.

Costs for traditional inspections were collected from SME input via phone survey. As with the classification step above, any SME who participated was promised anonymity in the recording of their input. The phone interview used for collection focused on gathering estimates of current tasking as experienced in the Appalachian region. Figures sought were per tasking lists of current necessary equipment, average time to conduct an inspection, approximate time needed to create a report, and expected site length. From these reported figures, an average inspection speed of 1.61 kilometers per hour (1 mph) was established, which is reasonable when considering the impact of terrain on known average walking speeds (Murtagh et al., 2021). Additionally, inquiries into the approximate pay rate for a pipeline inspector on a per hour basis set an expectation of $20/hr for this financial analysis.

Creating the realized cost standardization of $/km required the defining of a collection scenario to which the factors of both methods could be applied. The accuracy assessment study area was selected, as its usage would allow the direct application of the UAV inspection recorded time data. Annual cost amortization to total kilometers inspected at this site required the scenario to include total inspections conducted at this site. For the scenario to be as accurate as possible, the inspection schedule of the GWPCP was applied (West Virginia Department of Environmental Protection, 2013), which outlines weekly and weather inspections, which occur after 0.25 inches of precipitation. For the immediate region of the study site, the average number of precipitation events meeting this criterion annually was determined from the last 3 years climate data, as recorded in the Global Surface Summary of the Day (GSOD) dataset (User Engagement and Services Branch, 2022). Combining the weekly and average weather

determined inspections for a year, and multiplying by the study area length, gave the total space to be inspected. Finally, expected lifespan of single expenditure items were determined from the following equation:

$$Y = \left(\frac{H}{F}\right)/A$$

Where *Y* is the number of years to be expected from an item, *H* is the expected life of an item in flight hours, *F* is the flight time per kilometer as recorded during collection, and *A* is the number of inspections per year. As the multispectral sensor is designed for integration into the UAV's mount, the determined lifespan (*Y*) was applied to this item as well in cost calculations. With all of these portions calculated, $/km estimates were produced for each method.

An element of flexibility was then entered into the cost calculations each of the inspection methods to broaden the perspective of the impact of changing the input factors on the resultant costs. Terrain of varying difficulty is likely to be encountered by an inspector in Appalachia performing traditional pipeline inspections. As such, cost analyses were conducted for variable inspector speeds, ranging from 0.25 mph to 2 mph in 0.25 mph steps. Similarly, flexibility analysis assumed that improvements are likely to be seen with several portions of the drone inspection process. The first aspect adjusted for was an optimized collection. In this flexibility scenario, the frequent inspections of the site would reasonably lead to a more streamlined set up and flight of the UAV at the study site, shortening total time per inspection. Moreover, the usage of optimized data transfer and storage technologies can reduce the transfer time necessary, leading to a reduced time necessary of the UAV pilot. Further, a general processing optimization was included, to offer a flexible view of the impact which might be seen with improved GIS hardware and software. As there are many difficult to quantify computational

variables which can result in improved processing, the analysis as conducted was used as a baseline, and processing times were reduced up to 70% in 10% increments.

## Results

### Validation Plot Statistics

Across the 30 AAPS, there was a mean residual distance of 0.075 m (SE = 0.009 m) between the two datasets, suggesting a relatively high alignment between the two products. Digitization of the painted ground plots created a sample set with a mean area of 0.90 $m^2$ (n=30, SE = 0.02 $m^2$). SME classification of these plots resulted in passing and failing plots numbering 12 and 13, respectively. Passing plots had a mean extracted area of 0.85 $m^2$ (SE = 0.04 $m^2$) and the failing class had a mean of 0.96 $m^2$ (SE = 0.03 $m^2$). SME review found 5 sample plots to be indeterminate, and they were excluded from the validation accuracy assessment. Digitized training data for SVM creation had a mean area of 3.66 $m^2$ (n = 120, SE = 0.33 $m^2$). Passing and failing training plots had an average area of 4.09 $m^2$ (n = 60, SE = 0.53 $m^2$) and 2.41 $m^2$ (n = 60, SE = 0.31 $m^2$) respectively.

### Model Classification Accuracy

The validation plots for the multispectral SVM model had an overall accuracy of 92.00% (Table 1). Accurately classified passing validation plots had an average modeled vegetation coverage of 91.87% (n = 12, SE = 3.05%). Accurate failing plots had an average modeled vegetation coverage of 14.45% (n = 11, SE = 4.60%). The two incorrectly classified plots were both identified as failing by the SME. The vegetation coverage for these two misclassified plots was consistently high, with a mean of 97.77% coverage (SE = 0.73%). For the whole model, the

user accuracies were 85.71% and 100% for passing and failing respectively. Conversely, the producer's accuracies were 100% and 84.62% for passing and failing. Overall, the model produced a kappa of 0.8408.

All accuracy values of the RGB model exactly matched the validation values of the multispectral model, such as an overall accuracy of 92.00% was achieved by the RGB model (Table 2). Differences were seen in specific coverage in each model. Validation plots accurately classified as passing had an average modeled vegetation coverage of 95.40% (n = 12, SE = 2.60%), and accurately classified failing plots had an average modeled vegetation coverage of 16.73% (n = 11, SE = 5.76%). This model misclassified the same two validation plots as the multispectral model, which were both identified as failing by the SME. In the RGB SVM model, the vegetation coverage for these two misclassified plots was once again high, with a mean of 99.60% coverage (SE = 0.42%). The user accuracies were the same at 85.71% and 100% for passing and failing respectively. Similarly, the producer's accuracies were the same at 100% and 84.62% for passing and failing. Overall, the model produced the same kappa of 0.8408.

## Financial Analysis

In the region containing the study area, there were 182 total rain events greater than 0.25 inches for 2019, 2020, and 2021, setting the number of average weather inspections to 61. From this a total of 113 total inspections were projected for this study area. Each inspection was flown in two branches, meaning the total number of inspection flights at this site would be 226 annually. Expert input placed UAV lifespan to be 1,000 flight hours before costly maintenance leads to a likely replacement of the drone system. With each flight in the study area covering

approximately 1 km in a period of 20 minutes of flight, the drone would be expected to last 13.25 years until replacement was required.

Using the original flight data and processing times from this analysis, drone inspections had a cost of $194.34/km (Table 3), which was significantly larger than the $46.12/km calculated for the traditional inspections (Table 4). The minimal equipment of the traditional inspections resulted in a small proportion of the final expense at 6% (Figure 8) while the manpower requirements accounted for the majority of the expenses. Despite the increased cost and number of pieces of equipment required for the UAV inspections, equipment only accounted for 7% of the total per kilometer cost. The licenses required for the GIS analysis accounted for 14% of the total at $27.99/km. The remainder of the UAV inspection cost, and the largest portion of the total, was the manpower costs at $153.33/km (Figure 8).

UAV manpower costs were over 3.5 times greater than the traditional inspection manpower cost of $43.57/km. The largest portion of overall drone inspections cost was the GIS analyst, which accounts for $121.25/km, or 62% of the total. In creating the dataset, the surface model, analysis of the model and report generation, the GIS analysis must spend a total of 2.43 hrs/km (Table 5). Projected reductions in processing times from a hypothetical increase in processing efficiency were generally unable to produce comparable costs to traditional methods, with exceptions being noted at and above 50% time reductions when compared to the slowest hypothesized traditional inspection speed of 0.25 mph (Table 6). At 50% reduction and 0.25 mph, costs were within 5% of each other, favoring the traditional method. The assessment of additional hypothesized drone inspection price reduction through flight optimization found a pilot time reduction of 51.6%, from 1.28 hrs/km to 0.62 hrs/km (Table 7). This reduction lowered the UAV inspection manpower costs 10.9%, to $136.67/km (Figure 8). Including this

optimized flight, comparable costs were again only seen at the lowest traditional inspection speed of 0.25 mph, though now only 30% processing optimization was required (Table 8). Further, a greater overhead cost for pipeline inspectors of 40%, in line with some higher estimates from the US SBA, reduced the cost difference seen between the two methods, where costs became comparable at a 0.25 mph traditional inspection speed against a 5% GIS processing increase (Table 9).

## Discussion

### Inspection Comparison

The accuracy assessments of both models suggest the ability of either multispectral or RGB equipped UAVs to provide pipeline vegetation inspections at reasonably high accuracy compared to current standards. Both datasets sharing the same accuracy is surprising, as previous studies typically find one sensor to outperform the other (Carabassa et al., 2020; Grybas and Congalton, 2021; Zheng et al., 2020). From the results, it appears that the technique is promising, and SVM does appear to be an appropriate classification approach at this small spatial resolution. Several points of concern do remain, which likely warrants further evaluation of this technique.

Of central concern is the fact that both dataset models misclassified the same two plots, ground samples 24 and 26. These two plots had different vegetation patterns from each other and were each unique in their own way from the rest of the validation plots. Plot 24 was noted to be marginal but failing during SME classification (Figure 9). Vegetation across this plot was rather evenly distributed, and no soil was visible inside the plot. The reason noted for this plot to be labeled failing in SME classification was the broad presence of erosion control netting in the areas between visible vegetation. Construction efforts often use this type of material to cover

bare earth it protects the surface layer of the soil from direct rain exposure, protects the complete displacement of applied seeds, offers some stability to the soil beneath, and is typically biodegradable, thus requiring minimal future maintenance. As noted by an SME, it is common to see this material on pipeline construction operations upon steep and otherwise difficult to revegetate surfaces. As this material is a permeable impermanent cover, inspectors treat it as bare earth in their assessments, leading this plot to be considered failing.

The material used at this site was made of a twine type netting interwoven with straw. Being vegetation derived materials, they were likely a significant contributor to the failure seen in both models. While there are spectral differences between living vegetation and dried vegetative material, those nuances were not adequately captured in the SVM's training dataset. Moreover, pipeline inspectors note that the presence of dry vegetation itself is not enough to fail a plot, and a more complete view of vegetation health must be taken for a proper assessment. Future studies concerned with inaccurately identifying erosion control should consider the creation of a third class of ground cover comprised of dry vegetation. While not yet assessed from our data, the hope is that areas of dry vegetative material would be flagged for further inspection without indicating them as outright failing or passing. Further, SVM may need to be evaluated against other machine learning models should a third class be created, as SVM is essentially binary in its classification design (Sheykhmousa et al., 2020).

Unlike plot 24, plot 26 did present bare soil in significant enough quantities as to be deemed failing (Figure 10). The form of the vegetation was larger and more clumped than plot 24, but the likely cause of misclassification is high soil moisture. Plot 26 was located downhill of a water seep which forms a marsh-like area on the pipeline. Water is noted for high spectral absorbency in the visible and NIR ranges of light, in turn reducing the soil reflections from this

plot. Detecting high soil moisture is possible in remote sensing with the collection of thermal data and calculation of NDVI from a site (Zeng et al., 2004), and would aid in avoiding this issue in the future. Sensors with simultaneous capture of thermal and multispectral data are not commonly available, with options like the Sentera 6x Thermal arriving on the market only recently. Future studies with access to such sensor technologies should consider conducting a soil moisture calculation for inclusion in surface modeling.

Land access limitations also reduced the assessment strength of this study. With 30 validation plots established, 25 of which were suitable for analysis, a limited range of site conditions was sampled. Further, landscape variability is untested, as only 15% of study area was available for validation plots. Varied soils are found in the study area and its immediate surroundings, with 21 different soil units being identified by the Natural Resource Conservation Service (NRCS) Web Soil Survey (Natural Resource Conservation Service, 2019). As found in previous research, varied soils produce unique spectral returns (Meerdink et al., 2019; Baldridge et al., 2009). Moreover, soil-type variability could also be impacted on pipelines due to the significant disturbance and mixing of soils which occurs during construction. Vegetation species variability can also confound spectral returns (Kokaly et al., 2017). Ultimately, additional samples would provide a better depiction of the accuracy and limitations of this technique.

Another significant improvement in analysis of this type could occur with the integration of GIS data reflecting permit areas and management actions. All assigned boundaries of areas included and excluded for analysis and modeling are based on heads-up digitization. As such, there is the possibility that areas not intended to be included in inspections were used for either training or validation. Further, areas with their own management actions, like areas with erosion matting or wetland presence, can be evaluated separately. Being granted access to this data may

enable the subdivision of models into management units, where more accurate models can be created for known surface conditions.

Financial Analysis

The financial analysis of our study's scenario suggests that the tested UAV pipeline inspection approach will be fiscally difficult to implement in all but the most complex terrain. From the factors included, the analysis suggests that the traditional inspection approach, using a simple equipment set and lower inspector pay rate, is likely to produce lower costs than the UAV approach per kilometer. The greatest individual cost in the UAV inspection method was the projected cost of the GIS analyst. As a manpower factor, this will be difficult to avoid, though it is reasonable to expect that future operations may be able to reduce the time spent performing GIS analysis per kilometer. As UAV efficiency increases, inspection costs become more comparable to traditional inspections (Figure 11).

The scenario used for analysis is likely an overly generalized representation of the final form a UAV pipeline inspection might take. Future research focused on method optimization will likely produce an inspection scheme which better capitalizes heretofore unquantified drone benefits. One such unaccounted benefit is the reduction in inspection time per kilometer between the drone and traditional inspection approaches. Even the unoptimized flight process reduced per kilometer time by 30%. This time reduction per site may enable the inspection of more sites in a single day. As the current scenario was formed using the study area and expected annual inspections thereupon, overall mission wide multisite productivity increases from a single inspector over a single day remain an unrealized element. Exploration of these time reductions can be accomplished in future studies with the creation of a larger dataset of traditional and UAV

inspections across multiple sites. Reasonable expectations would suggest that should UAV inspections consistently produce a reduced on-site time compared to traditional inspections, implementation of the technology would enable the same number of employees to inspect a larger quantity of sites for the same amount of work hours.

UAV inspections in this study did not undergo a time reduction optimization for collection and data transmission. The drone used, a DJI M-200 v2 quadcopter, is a general use drone capable of accepting a wide range of sensors, making it an optimal choice for research and evaluation of various technologies. Quadcopter drones, however, can be outperformed by purpose-built drones with higher speed fixed wing flight, integrated multispectral collection, or longer flight times. As the flight optimization used in this analysis is based off of the published capabilities of the DJI M-200 v2, it is reasonable to suspect that another currently available drone may outperform these figures. Of the same thread, the GIS processing used in this study was following common research practices on general purpose computing machines. The hypothetical optimization figure used in this study generally reduces processing times to address gross potential improvements from the technological optimization of hardware and software used. Due to the nature of specialized computing suites, it would be unsurprising to find a purpose-built suite capable of further reducing the time needed of a GIS analyst in the UAV inspection process. Optimization may also find some steps used in our analysis, like the manual assigning of ground control points during dataset construction, may not be needed to produce pipeline inspection reports of the desired quality and format.

The tested financial analysis scenario may also contain unaccounted factors creating cost errors in favor of UAV inspections. The use of civilian and commercial drones in the US are governed under a regulation set known as the Part 107 – Small Unmanned Aircraft Systems

regulations (Federal Aviation Administration, 2016). In these rules, §107.31 mandates that UAVs remain within the line of site of the flight team throughout any operations. Should a drone's flight path be visually obstructed, flight crews can deploy a drone observer afield with a reliable means of communicating with the flight team. It is possible to seek a waiver from the Federal Aviation Administration to excuse this requirement, but lacking a waiver, UAV inspections may require increased manpower costs on some sites. Additionally, technology limitations may also diminish the total distance covered by a drone. Drone missions loaded through a mission planning software, such as the UgCS client used in this study, pre-load a series of waypoints which the drone will follow, even if it loses connection with a ground controller station. Though the flight is thusly set, many drone operating systems will instruct a midmission return to take-off location if they cannot re-establish communication with the controller after a hard-set period of time. Different manufacturers use various periods of time, so post-signal lost collection will be heavily dependent on the equipment selected for the mission. Signal loss may also vary from day to day at the same site, as many as many environmental factors from humidity to foliage to sunspot activity will all impact signal attenuation. Finally, unlike traditional inspectors, drones are generally incapable of conducting a pipeline inspection in precipitation or extreme cold. The downtime created by a location's annual climate will hinder UAV usage to a currently unquantified degree. These unquantified factors can all lead to increased costs not included in this financial analysis. These factors can likely be addressed in future studies through a more thorough equipment evaluation, included assessment of the current FAA waiver process, and efforts to assess the impacts of annual climate.

Traditional inspections contain variables and unknowns that will need to be addressed in future studies. One of the greatest sources of error is likely found in the self-reporting of

traditional inspection efficiency. An economics performance assessment study found that self-reporting of performance may not accurately represent objective performance (Pransky et al., 2006). Moreover, the method with which a self-reporting survey is conducted is of high importance to the data's accuracy (Peters et al., 2000; Stewart et al., 2000). Further, the given financial analysis does not include a precise capture of overhead costs for the traditional pipeline inspector and may be grossly inaccurate. Though the base rate of overhead noted by the US SBA is 25%, with a common maximum of 40% (Weltman, 2019), these datapoints do not specifically represent hazardous work, such as that which is conducted on pipelines. On many fully installed and operational sites, pipeline inspectors are expected to wear flame resistant gear, high visibility markers, hardhats, and steel toed boots. This gear suggests a hazardous exposure to employees, which may cause employer costs, such as insurance, to be far more expensive than a standard overhead amount would address. Future studies should gather more accurate data of traditional performance and overhead cost factors to better represent the true cost of the common inspection approach.

Finally, the data created from each of these inspection processes is very different, thus the recording and analysis benefits of the UAV approach is difficult to quantify against a traditional approach. Drone collection creates a complete surface model of the site, containing fixed coordinates and time metrics. Traditional inspections, while capable of addressing the finer detail at some locations, lack a complete capture product, and instead provide limited data which the inspector determined to be pressing. While much of these data appear to be extractable from a GIS dataset, as shown in the accuracy assessment portion of this study, UAV inspections make wide computational assessments of the entire site possible. Potential products include the ability to identify and assess whole site issues, such as an underperforming seed mix, and surface

change at any location can be evaluated over time, which enables improved assessment of management actions. Should the addition of these type of products increase the industry valuation of UAV inspections, the increased costs of performing a UAV inspection would be offset by the value of the products delivered.

## Conclusions

The Marcellus and Utica shale plays in the Appalachian basin have seen significant growth in unconventional NG production. Installation of the required midstream infrastructure disturbs long tracts of difficult to traverse land which can cause significant ecological impact if not managed. Regulations have been created to guide site inspections, which are heretofore completed afoot. Inspectors traversing these stretches hike across difficult terrain, creating both health and safety concerns. A key aspect to these inspections is the assessment of vegetation re-establishment across the permit area. UAVs have been implemented across various industries due to their speed, size, and collection capabilities. Our study begins the evaluation process and lays foundational expectations of UAV capabilities as compared to traditional approaches in the energy industry.

Both RGB and multispectral sensors, which represent a wide range of available sensors, were evaluated for use. The multispectral sensor allowed the inclusion of an NDVI dataset, but this did not appear to improve performance when evaluating SME classified plots. SVM models derived from each sensor set performed equally high, with both models producing erroneous classification on the same 2 plots. These 2 plots contained unique ground conditions not yet modeled for, suggesting the need for future inclusion of an additional class, or use of a thermal

sensor. Increased land access and accuracy assessment can provide a more robust evaluation of this emergent technique.

While unable to replicate current inspectors at fine ground detail, a likely implementation of this technique can occur in ongoing management actions. Though current analysis shows UAV based inspections to be more costly than traditional approaches, the evaluation of additional identified factors may create a more complete picture of the relationship between these two techniques, and aid in reducing this cost differential. After determining effective performance and cost optimization, a purpose-built drone could be deployed over a pipeline stretch using a previously created flight plan on a regular basis. From this, models of a reasonably high accuracy are derived, which could in turn be used to identify larger issues requiring immediate responses. This tasking could cover some weekly and post-rain inspections, where there is a time sensitive nature to detecting large failures. Trained and certified professionals will still be needed in inspections, as they can seek-out conditions which the drone may miss; however, their time spent traversing difficult terrain would be reduced. On such terrain, both worker safety and cost savings may be realized. Thus, the inclusion of UAVs in pipeline inspection procedures appears to be a promising enterprise.

**Literature Cited**


Alley-Young, G. 2020. Drone (Unmanned aerial vehicle). Salem Press Encyclopedia

Baldridge, A. M., S. J. Hook, C. I. Grove and G. Rivera. 2009. The ASTER Spectral Library Version 2.0. Remote Sensing of Environment. 113: 711-715. https://doi.org/10.1016/j.rse.2008.11.007

Campbell, J. B., and R. H. Wynne. 2011. Introduction to remote sensing. 5th ed. New York, NY: Guilford Press

Carabassa, V., P. Montero, M. Crespo, J. C. Padró, X. Pons, J. Balagué, L. Brotons, and J. M. Alcañiz. 2020. Unmanned aerial system protocol for quarry restoration and mineral extraction monitoring. Journal of Environmental Management. 270: 110717. https://doi.org/10.1016/j.jenvman.2020.110717

Cederholm, C. J. and L. C Lestelle.1974. Observations on the effects of landslide siltation on salmon and trout resources of the Clearwater River, Jefferson County, WA, 1972-73, Final Report. University of Washington

Doman, L., and A. Kahan. 2018. United States remains the world's top producer of petroleum and natural gas hydrocarbons. US Energy Information Administration, 21. Available at: https://www.eia.gov/todayinenergy/detail.php?id=36292. Accessed 12 April 2022

Esri. 2021. ArcGIS Pro 2.9.2. Redlands, California

Federal Aviation Administration. 2016. Part 107 - Small Unmanned Aircraft Systems, 49 U.S.C. 106(f) § 107

Grybas, H., and R. G. Congalton. 2021. A Comparison of Multi-Temporal RGB and Multispectral UAS Imagery for Tree Species Classification in Heterogeneous New Hampshire Forests. Remote Sensing. 13: 2631. https://doi.org/10.3390/rs13132631

Hallermann, N., and G. Morgenthal. 2014. Visual inspection strategies for large bridges using Unmanned Aerial Vehicles (UAV). In Proceedings of the 7th International Conference on Bridge Maintenance, Safety and Management (IABMAS). 661-667

Kargbo, D. M., R. G. Wilhelm, and D. J. Campbell. 2010. Natural gas plays in the Marcellus shale: Challenges and potential opportunities. Environmental Science and Technology. 44: 5679–5684. https://doi.org/10.1021/es903811p

Kemp, P., D. Sear, A. Collins, P. Naden, and I. Jones. 2011. The impacts of fine sediment on riverine fish. Hydrological processes. 25: 1800-1821. https://doi.org/10.1002/hyp.7940

Kim, J., S. Kim, C. Ju, and H.I. Son. 2019. Unmanned aerial vehicles in agriculture: A review of perspective of platform, control, and applications. IEEE Access. 7: 105100-105115. doi: 10.1109/ACCESS.2019.2932119

Kokaly, R. F., R. N. Clark, G. A. Swayze, K. E. Livo, T. M. Hoefen, N. C. Pearson, R. A. Wise, W. M. Benzel, H. A. Lowers, R. L Driscoll, and A. J. Klein. 2017. USGS Spectral Library Version 7: U.S. Geological Survey Data Series. 1035: 61. https://dx.doi.org/10.5066/F7RR1WDJ

Langlois, L. A., P. J. Drohan, and M. C. Brittingham. 2017. Linear infrastructure drives habitat conversion and forest fragmentation associated with Marcellus shale gas development in a forested landscape. Journal of Environmental Management. 197: 167-176. https://doi.org/10.1016/j.jenvman.2017.03.045

Liu, P., K. K. R. Choo, L. Wang, and F. Huang. 2017. SVM or deep learning? A comparative study on remote sensing image classification. Soft Computing. 21: 7053–7065. https://doi.org/10.1007/s00500-016-2247-2

Marcellus Drilling News. 2021. SWPA Olympus Well Becomes Longest Marcellus Onshore Lateral. Available at: https://marcellusdrilling.com/2020/12/swpa-olympus-well-becomes-longest-marcellus-onshore-lateral/. Accessed 12 January 2022

Meerdink, S. K., S. J. Hook, D. A. Roberts, and E. A. Abbott. 2019. The ECOSTRESS spectral library version 1.0. Remote Sensing of Environment. 230: 1–8. https://doi.org/10.1016/j.rse.2019.05.015

Messersmith, D., D. Brockett, and C. Loveland. 2015. Understanding natural gas compressor stations. Penn State Extension. Available at: https://extension.psu.edu/understanding-natural-gas-compressor-stations. Accessed 05 January 2022

Murtagh, E. M., J. L. Mair, E. Aguiar, C. Tudor-Locke, and M. H. Murphy. 2021. Outdoor Walking Speeds of Apparently Healthy Adults: A Systematic Review and Meta-analysis. Sports Medicine. 51:125-141. doi: 10.1007/s40279-020-01351-3

Natural Resources Conservation Service. 2019. Web Soil Survey. Available at: http://websoilsurvey.sc.egov.usda.gov/. Accessed 14 January 2022

Nikolic, J., M. Burri, J. Rehder, S. Leutenegger, C. Huerzeler, and R. Siegwart. 2013. A UAV system for inspection of industrial facilities. In 2013 IEEE Conference on Aerospace Conference: Big Sky, MT. 1-8

Olmstead, S. M., L. A. Muehlenbachs, J. S. Shih, Z. Chu, and A. J. Krupnick. 2013. Shale gas development impacts on surface water quality in Pennsylvania. Proceedings of the National Academy of Sciences of the United States of America. 110: 4962–4967. https://doi.org/10.1073/pnas.1213871110

Peters, M. L., M. J. Sorbi, D. A. Kruise, J. J. Kerssens, P. F. M. Verhaak, and J. M. Bensing. 2000. Electronic diary assessment of pain, disability and psychological adaptation in patients differing in duration of pain. Pain. 84: 181-192. https://doi.org/10.1016/S0304-3959(99)00206-7

Popova, O. 2017a. Marcellus Shale Play: Geology Review. U.S. Energy Information Administration. Available at: https://www.eia.gov/maps/pdf/MarcellusPlayUpdate_Jan2017.pdf. Accessed 03 January 2022

Popova, O. 2017b. Utica Shale Play: Geology Review. U.S. Energy Information Administration. Available at: https://www.eia.gov/maps/pdf/UticaShalePlayReport_April2017.pdf. Accessed 03 January 2022

Pransky, G., S. Finkelstein, E. Berndt, M. Kyle, J. Mackell, and D. Tortorice. 2006. Objective and self-report work performance measures: a comparative analysis. International Journal of Productivity and Performance Management. 55: 390-399. https://doi.org/10.1108/17410400610671426

Richards, C., and K. L. Bacon. 1994. Influence of fine sediment on macroinvertebrate colonization of surface and hyporheic stream substrates. The Great Basin Naturalist. 54: 106-113. Available at: http://www.jstor.org/stable/41712819. Accessed 12 April 2022

Sabat-Tomala, A., E. Raczko, and B. Zagajewski. 2020. Comparison of Support Vector Machine and Random Forest Algorithms for Invasive and Expansive Species Classification Using Airborne Hyperspectral Data. Remote Sensing. 12: 516. https://doi.org/10.3390/rs12030516

Sheykhmousa M., M. Mahdianpari, H. Ghanbari, F. Mohammadimanesh, P. Ghamisi and S. Homayouni. 2020. Support Vector Machine Versus Random Forest for Remote Sensing Image Classification: A Meta-Analysis and Systematic Review. IEEE Journal of Selected Topics in Applied Earth Observations and Remote Sensing. 13: 6308-6325. doi: 10.1109/JSTARS.2020.3026724

Stewart, W. F., R. B. Lipton, K. B. Kolodner, J. Sawyer, C. Lee, and J. N. Liberman. 2000. Validity of the Migraine Disability Assessment (MIDAS) score in comparison to a diary-based measure in a population sample of migraine sufferers. Pain. 88: 41-52. https://doi.org/10.1016/S0304-3959(00)00305-5

Tucker, C.J. 1979. Red and photographic infrared linear combinations for monitoring vegetation. Remote sensing of Environment. 8: 127-150

U.S. Department of Energy. 2020. The Appalachian Energy and Petrochemical Renaissance: An Examination of Economic Progress and Opportunities. Available at: https://www.energy.gov/sites/prod/files/2020/06/f76/Appalachian%20Energy%20and%20Petrochemical%20Report_063020_v3.pdf. Accessed 03 January 2022

U.S. Energy Information Administration. 2021. Natural gas explained. Available at: https://www.eia.gov/energyexplained/natural-gas/. Accessed 03 January 2022

User Engagement and Services Branch. 2022. Global Surface Summary of the Day Dataset. National Climatic Data Center, NESDIS, NOAA, U.S. Department of Commerce. Available at: https://www.ncei.noaa.gov/access/search/data-search/global-summary-of-the-day. Accessed 8 July 2022

Warner, N., C. Christie, R.B. Jackson, and A. Vengosh. 2013. Impacts of shale gas wastewater disposal on water quality in western Pennsylvania. Environmental Science Technologies. 47: 11849-11857. https://doi.org/10.1021/es402165b

Weltman, B. 2019. How Much Does an Employee Cost You? U. S. Small Business Administration. Available at: https://www.sba.gov/blog/how-much-does-employee-cost-you. Accessed 12 July 2022

West Virginia Department of Environmental Protection. 2013. General Water Pollution Control Permit. Available at: https://dep.wv.gov/WWE/Programs/stormwater/csw/Documents/OG%20stormwater%20GP%203_10_15.pdf. Accessed 12 April 2022

West Virginia Department of Environmental Protection. 2016. Erosion and Sediment Control Best Management Practice Manual. Available at: https://dep.wv.gov/WWE/Programs/stormwater/csw/Documents/E%20and%20S_BMP_2006.pdf. Accessed 12 April 2022

Zeng, Y., Z. Feng, and N. Xiang. 2004. Assessment of soil moisture using Landsat ETM+ temperature/vegetation index in semiarid environment. IGARSS 2004 IEEE International Geoscience and Remote Sensing Symposium. 6: 4306-4309. doi: 10.1109/IGARSS.2004.1370089

Zheng, H., X. Zhou, J. He, X. Yao, T. Cheng, Y. Zhu, W. Cao, and Y. Tian. 2020. Early season detection of rice plants using RGB, NIR-G-B and multispectral images from unmanned aerial vehicle (UAV). Computers and Electronics in Agriculture. 169: 105223 https://doi.org/10.1016/j.compag.2020.105223

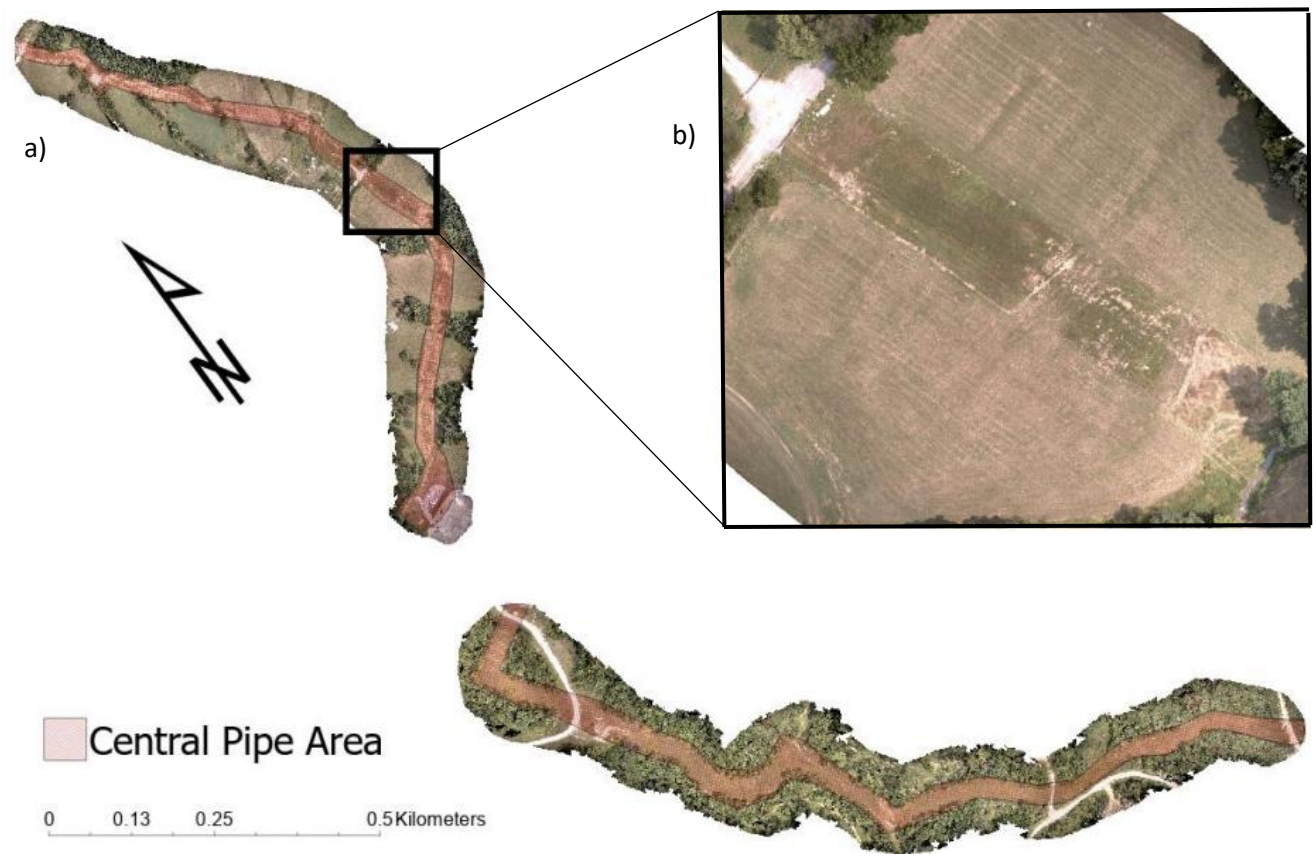


Figure 1. Approximately 2.3 km of natural gas pipeline used as study area for the UAV based evaluation of vegetation success in Northern West Virginia, USA. a) The full extent collected along the pipeline, with the area of vegetation assessment marked with red crosshatch. b) An expanded view of area enclosed in a) to enable a detailed view of the surface at the site. Note the surface variance in vegetation and disturbance in the linear pipeline area as compared to the surrounding agricultural field.

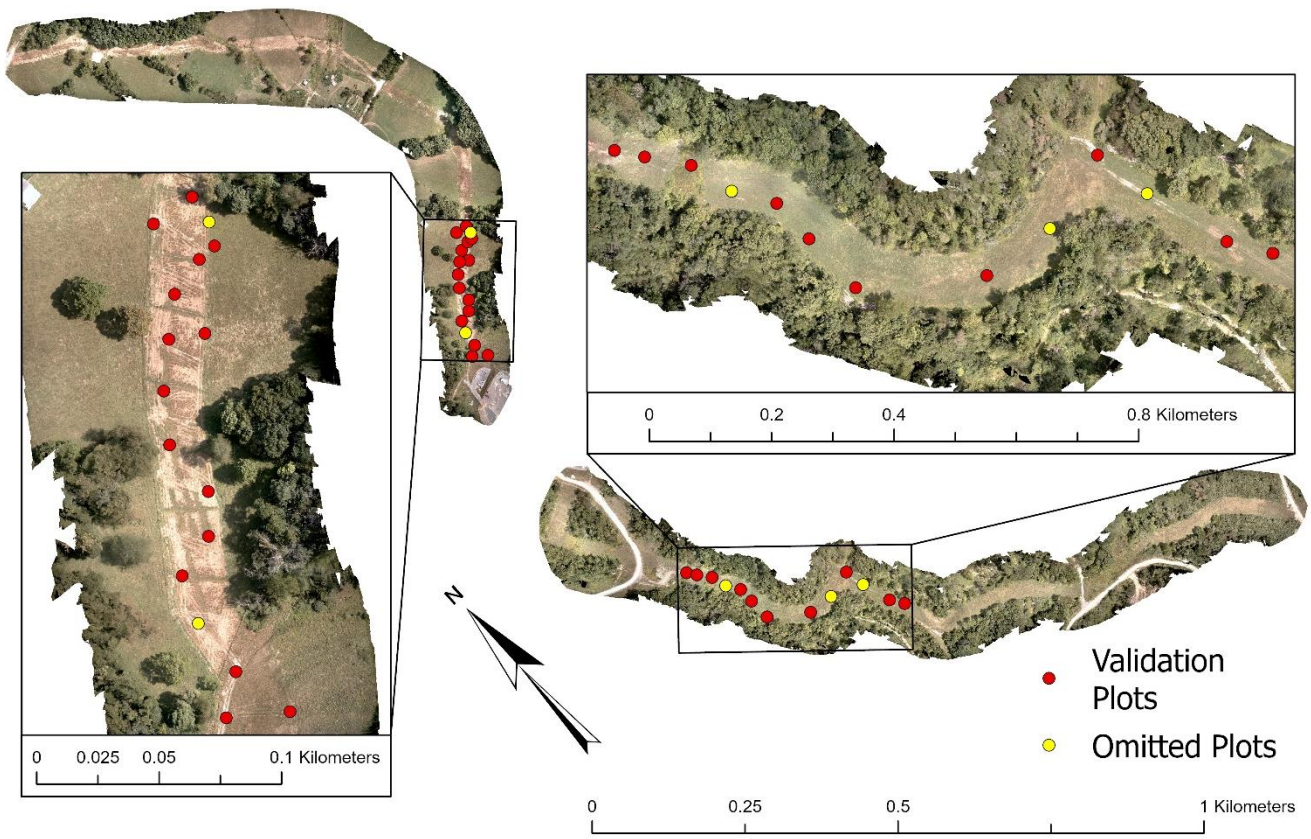


Figure 2. Location of the ground validation plots established in the study area. Inserts show each of the allowed access areas of the pipeline. Red indicates plots used for validation and yellow indicates omitted plots

Figure 3. Example of training plot established to denote areas on pipeline that failed vegetative cover threshold. Plot is approximately 1m square and used a 2-digit identifier outside the bottom right corner

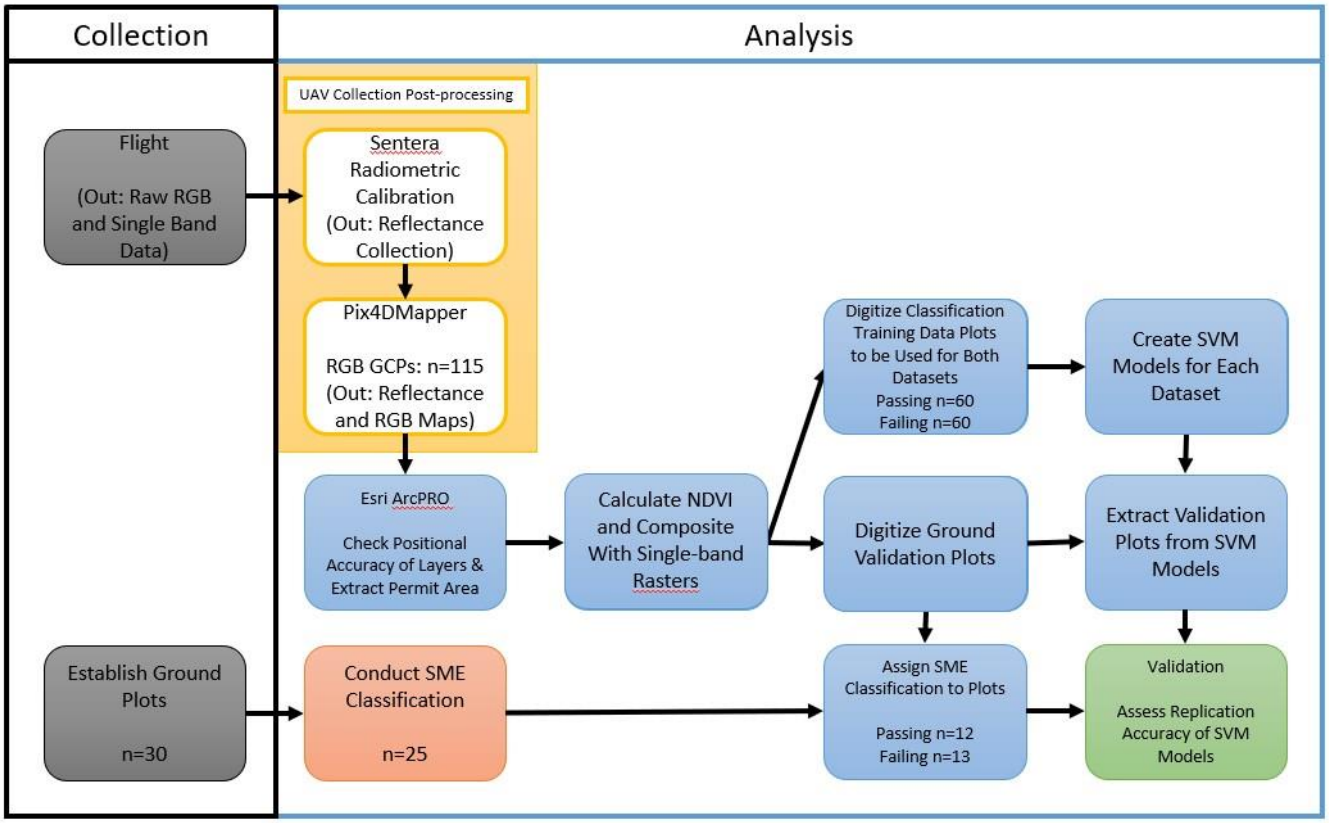


Figure 4. Workflow used to capture remote sensor data and ground sample points. Post-processing of the UAV data was conducted in two separate programs, with final analysis occurring in Esri ArcGIS Pro v2.9.2

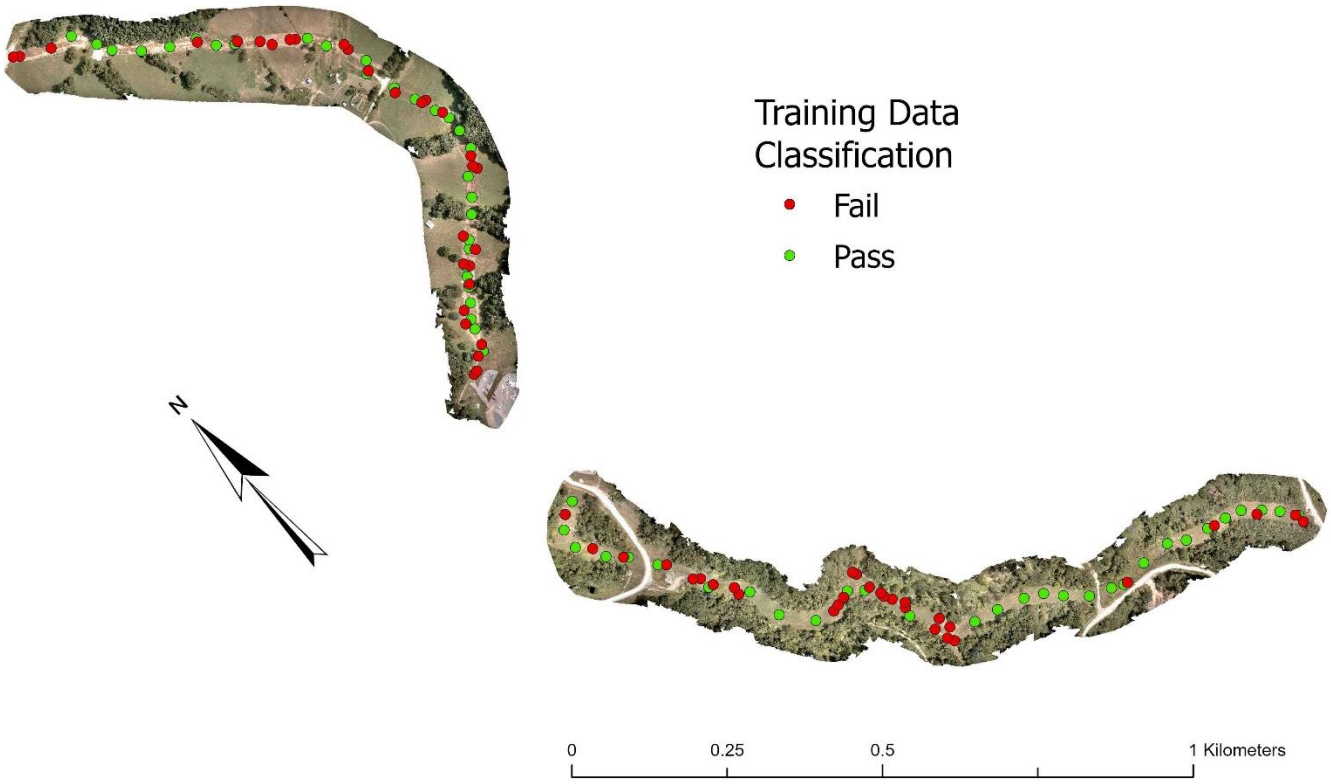


Figure 5. Manually digitized training data samples for SVM classification. Samples were created at a scale of 1:100. There were 120 samples created, 60 for each class, with 30 per class established in each branch of the pipeline.

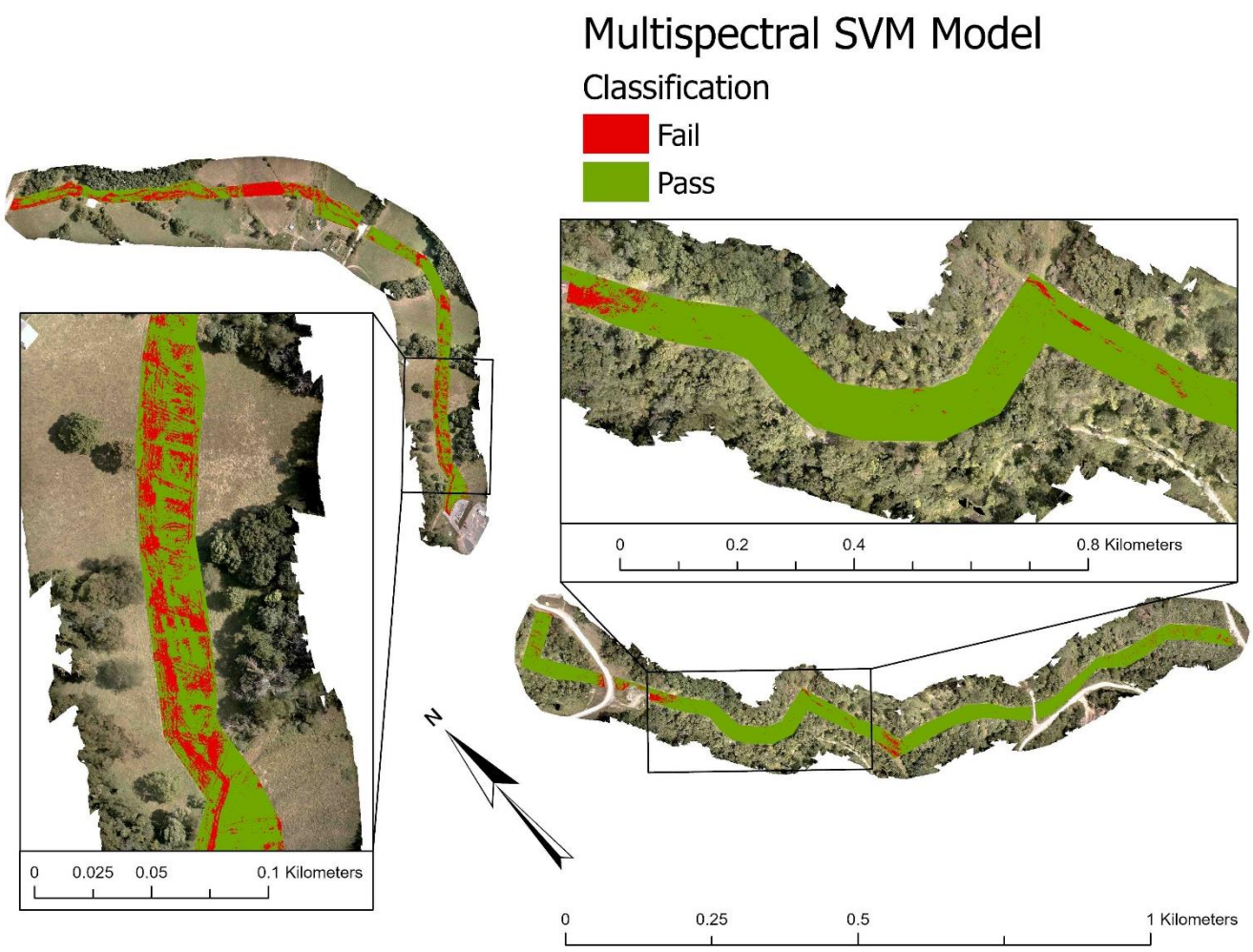


Figure 6. SVM classification model of the multispectral dataset using blue, green, red, and NIR bands with NDVI included. Green and red pixel color indicate passing or failing respectively as determined by the model. Inserts are included for a more detailed look at the extent available for validation plots. Spatial resolution of this model is 0.042 m.

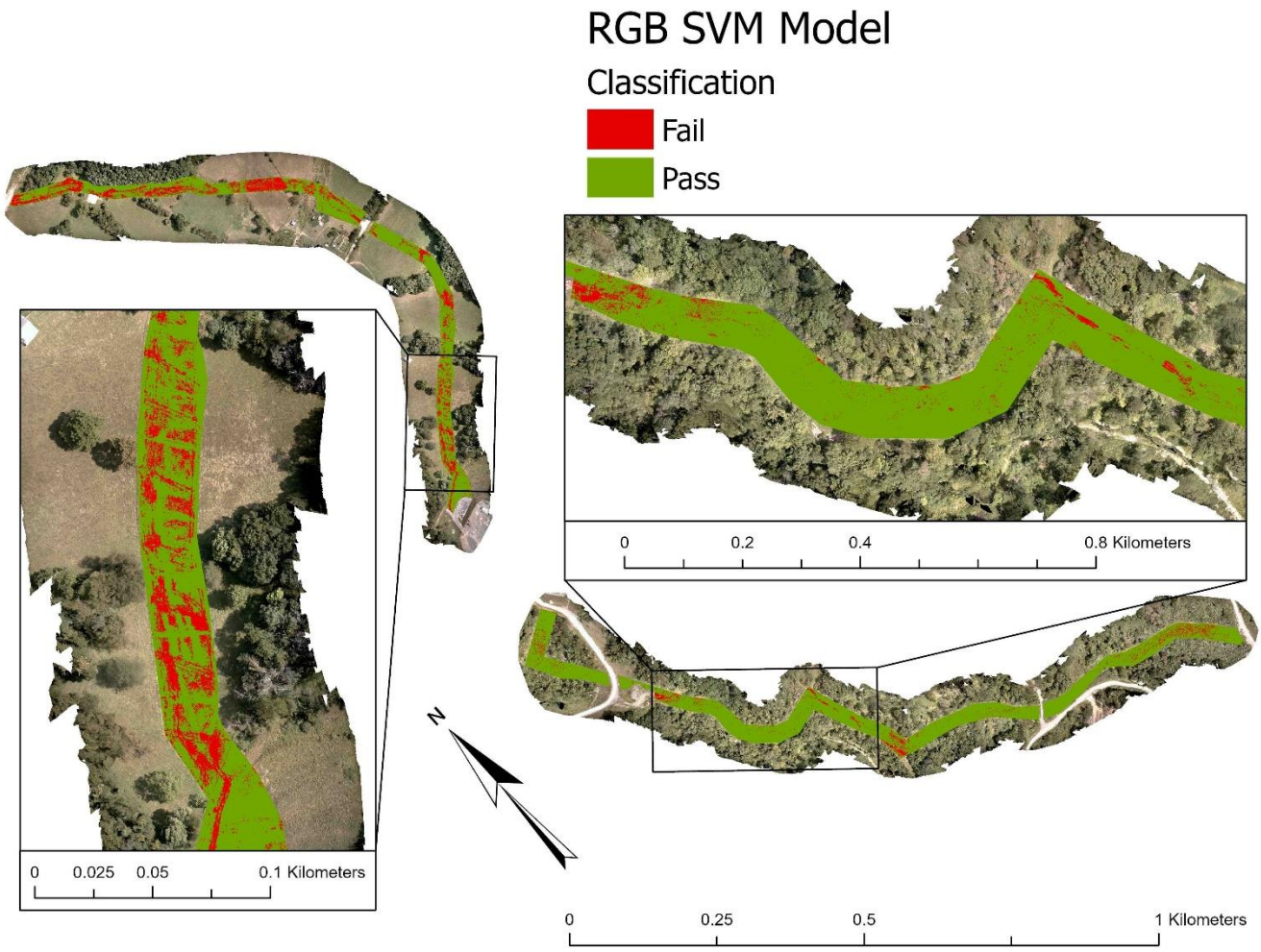


Figure 7. SVM classification model of the RGB dataset. Green and red pixel color indicate passing or failing respectively as determined by the model. Inserts are included for a more detailed look at the extent available for validation plots. Spatial resolution of this model is 0.063 m.

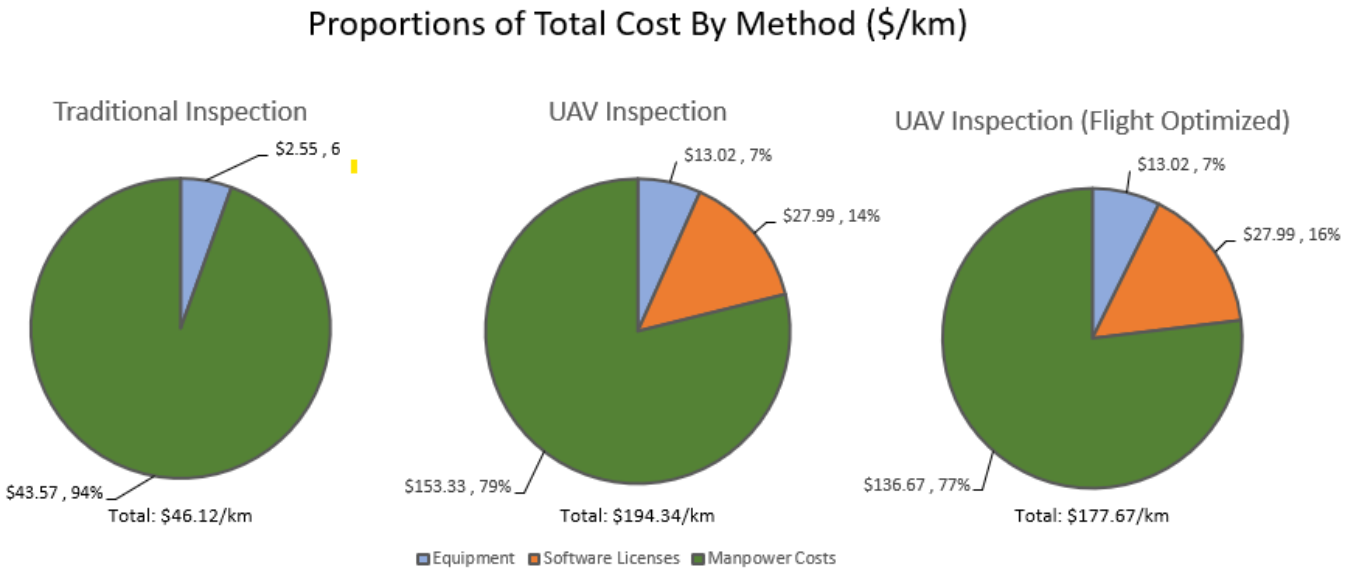


Figure 8. Charts depicting the proportion of each inspection method's cost categories. The three categories depicted are equipment, software licenses, and manpower in blue, orange, and green respectively. Total per kilometer costs are given below each chart.

Figure 9. A detailed image taken immediately after ground plot establishment of validation plot 24. This was one of two plots misclassified by both models. SME classification determined this plot to be failing due to the presence of straw-laden erosion control matting between the present vegetation.

Figure 10. A detailed image taken immediately after ground plot establishment of validation plot 26. This was one of two plots misclassified by both models. SME classification determined this plot to be failing, as there were large portions of soil present within the plot. Note the darker color of the soil, caused by high moisture content.

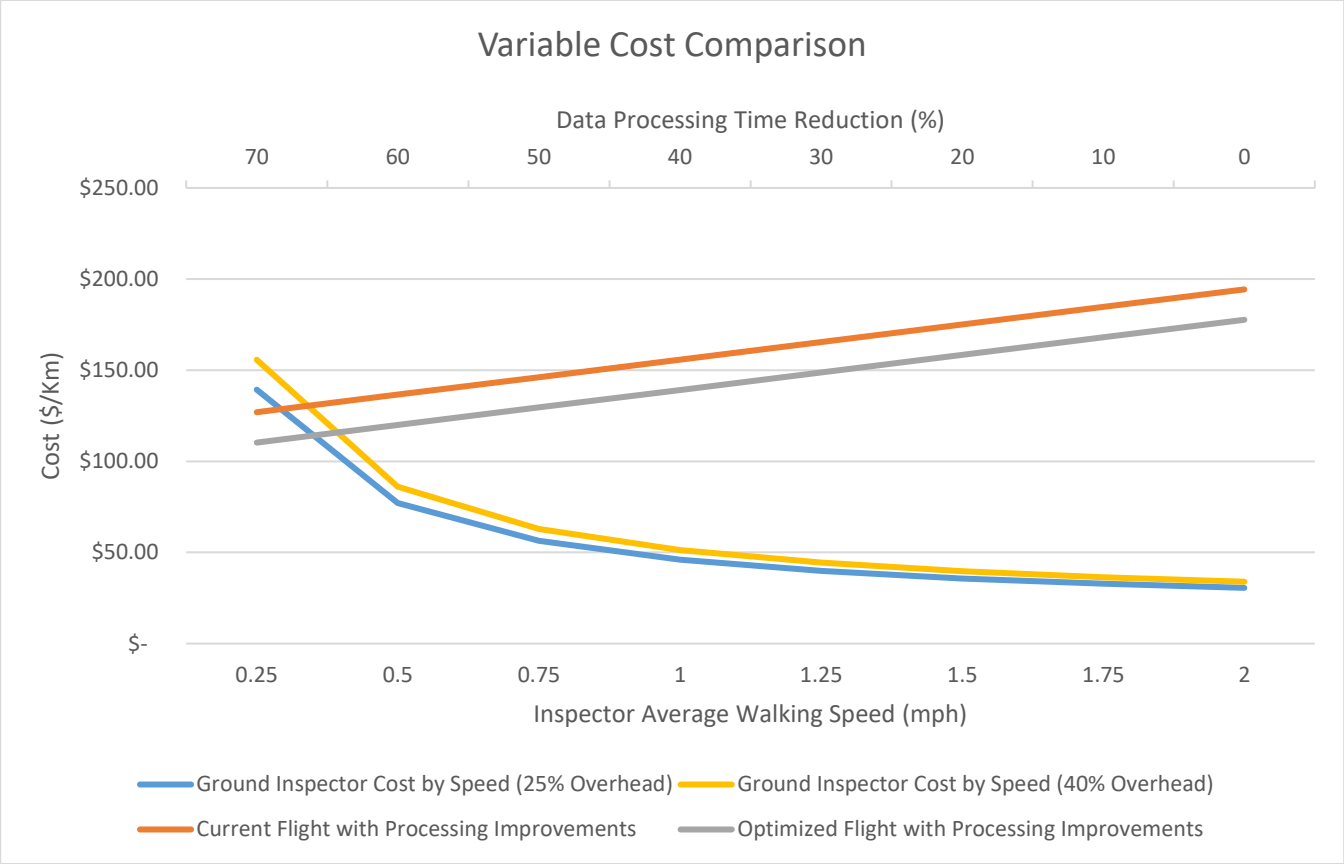


Figure 11. Cost trends per kilometer are shown including the variables of inspector speed and processing time reduction. Inspector speed is shown on the lower axis and increases from left to right. Data processing time reduction by percentage is shown on the upper axis and increases from right to left. Ground inspector plots show both a 25% overhead and 40% overhead in blue and yellow respectively. Similarly, drone cost with and without flight optimization are shown in grey and orange respectively. Note that the costs cross near 0.25 mph and 70% time reduction. This shows the point where cost per kilometer are lower using the drone inspection method.

Table 1. A confusion matrix between the True classification of the plots, as determined by the SME classification process, and the Predicted classification derived from the SVM model created from the multispectral dataset.

| | | True | | | |
|---|---|---|---|---|---|
| | | Fail | Pass | Totals | User Accuracy |
| Predicted | Fail | 11 | 0 | 11 | 1.0000 |
| | Pass | 2 | 12 | 14 | 0.8571 |
| | Totals | 13 | 12 | | |
| | Producer Accuracy | 0.8462 | 1.0000 | Overall Accuracy-> | 0.9200 |
| | | | | Kappa -> | 0.8408 |

Table 2. A confusion matrix between the True classification of the plots, as determined by the SME classification process, and the Predicted classification derived from the SVM model created from the RGB dataset.

| | | True | | | |
|---|---|---|---|---|---|
| | | Fail | Pass | Totals | User Accuracy |
| Predicted | Fail | 11 | 0 | 11 | 1.0000 |
| | Pass | 2 | 12 | 14 | 0.8571 |
| | Totals | 13 | 12 | | |
| | Producer Accuracy | 0.8462 | 1.0000 | Overall Accuracy-> | 0.9200 |
| | | | | Kappa -> | 0.8408 |

Table 3. A complete listing of projected costs to conduct a drone inspection in the study's scenario. Equipment costs are corrected first to annual cost, then cost per kilometer. Manpower costs are shown in hours per kilometer to cost per kilometer. Percent of total cost is shown in the right column.

| Drone Inspection | | | | | | | |
|---|---|---|---|---|---|---|---|
| Equipment Costs | | | | | | | |
| | Item/License | Cost ($) | Qty | Replacement Period (yrs) | $/yr | $/Km | % Of Method Total |
| | DJI M200 v2 | $ 6,000.00 | 1 | 13.25 | $ 452.83 | $ 1.71 | 1% |
| | Drone Insurance | $ 728.06 | 1 | 1 | $ 728.06 | $ 2.75 | 1% |
| | M200 Battery | $ 480.00 | 2 | 1.7 | $ 564.71 | $ 2.14 | 1% |
| | Sentera 6x Multispectral Sensor | $ 13,550.00 | 1 | 13.25 | $ 1,022.64 | $ 3.87 | 2% |
| | iPad | $ 599.00 | 1 | 1 | $ 599.00 | $ 2.27 | 1% |
| | Apple iCare | $ 149.00 | 1 | 2 | $ 74.50 | $ 0.28 | 0% |
| | Pix4d Mapper | $ 3,600.00 | 1 | 1 | $ 3,600.00 | $ 13.61 | 7% |
| | Esri ArcGIS Pro License | $ 3,800.00 | 1 | 1 | $ 3,800.00 | $ 14.37 | 7% |
| | | | | Equipment Cost Subtotal ($/Km) | | $ 41.00 | 21% |
| Manpower Costs | | | | | | | |
| | Position | Hourly Rate | Hourly Rate + 25% | | Hrs/Km | $/Km | |
| | Pilot | $ 20.00 | $ 25.00 | | 1.28 | $ 32.08 | 17% |
| | GIS Analyst | $ 40.00 | $ 50.00 | | 2.43 | $ 121.25 | 62% |
| | | | | Manpower Cost Subtotal ($/Km) | | $ 153.33 | 79% |
| | | | | Drone Inspection Cost Total ($/Km): | | $ 194.34 | |

Table 4. A complete listing of projected costs to conduct a traditional inspection in the study's scenario. Equipment costs are corrected first to annual cost, then cost per kilometer. Manpower costs are shown in hours per kilometer to cost per kilometer. Percent of total cost is shown in the right column.

| Traditional Inspection | | | | | | | |
|---|---|---|---|---|---|---|---|
| Equipment Costs | | | | | | | |
| | Item/License | Cost ($) | Qty | Replacement Period (yrs) | $/yr | $/Km | % Of Method Total |
| | iPad | $ 599.00 | 1 | 1 | $ 599.00 | $ 2.27 | 5% |
| | Apple iCare | $ 149.00 | 1 | 2 | $ 74.50 | $ 0.28 | 1% |
| | | | | Equipment Cost Subtotal ($/Km) | | $ 2.55 | 6% |
| Manpower Costs | | | | | | | |
| | Position | Rate ($/hr) | Rate + 25% ($/Hr) | | Hrs/Km | $/Km | |
| | Pipeline Inspector* | $ 20.00 | $ 25.00 | | 1.74 | $ 43.57 | 94% |
| | | | | Traditional Inspection Cost Total ($/Km): | | $ 46.12 | |

Table 5. Times of different collection and processing steps needed for drone collection. Times were first recorded in minutes and converted to hours. Corrections were then made hours needed to produce one kilometer of results. Drone pilot tasks are in the upper section, totaling in blue. Orange contains the GIS analyst subtotals, with the GIS analyst total in green.

| **Collection (Adjusted to min/Km)** | | |
|---|---|---|
| | Time (Min) | Time (Hr) |
| Set Up | 30 | 0.50 |
| Calibration | 2 | 0.03 |
| Flight | 20 | 0.33 |
| Moving Pics to Computer | 25 | 0.42 |
| **Pilot Total (Hr/Km):** | | 1.28 |

| **Processing (Adjusted to min/Km)** | | |
|---|---|---|
| | Time (Min) | Time (Hr) |
| Align | 45 | 0.75 |
| Set GCP | 30 | 0.50 |
| Products | 20 | 0.33 |
| Processing Subtotal (Hr/Km): | | 1.58 |
| **Modeling** | | |
| | Time (Min) | Time (Hr) |
| Load | 15 | 0.25 |
| Mosaic | 2 | 0.03 |
| Calculate NDVI | 1 | 0.02 |
| Clip | 1 | 0.02 |
| Check Training Features | 20 | 0.33 |
| Train SVM | 1 | 0.02 |
| Reclassify | 1 | 0.02 |
| Total | 41 | 0.68 |
| Modeling Subtotal (Hr/Km): | | 0.34 |
| **Analysis and Report Creation** | | |
| | Time (Min) | Time (Hr) |
| Analysis (Review) | 30 | 0.50 |
| Report | 30 | 0.50 |
| Total | 60 | 1.00 |
| Analysis and Report Subtotal (Hr/Km): | | 0.50 |

| | |
|---|---|
| **GIS Analyst total (Hr/Km):** | 2.43 |

Table 6. Proportionate comparison of the cost per kilometer, calculated as traditional / drone cost for the original flight times and inspector overhead costs. Proportionate comparisons are shown across variances in inspector walking speed and GIS processing time reductions achieved through more efficient computing. Traditional inspections are applying a 25% overhead. Results closer to 1 denote costs closer in similarity. Cells containing values with less than 10% difference, or which favor drone inspections are highlighted in green.

| | | $/Km Proportional Cost Comparison | | | | | | | | |
|---|---|---|---|---|---|---|---|---|---|---|
| | | Drone Processing Efficiency Increase | | | | | | | | |
| | | 0% | 5% | 10% | 20% | 30% | 40% | 50% | 60% | 70% |
| Inspector Speed (mph) 25% Overhead | 0.25 | 0.72 | 0.74 | 0.75 | 0.80 | 0.84 | 0.89 | 0.95 | 1.02 | 1.10 |
| | 0.5 | 0.40 | 0.41 | 0.42 | 0.44 | 0.47 | 0.50 | 0.53 | 0.57 | 0.61 |
| | 0.75 | 0.29 | 0.30 | 0.31 | 0.32 | 0.34 | 0.36 | 0.39 | 0.41 | 0.44 |
| | 1 | 0.24 | 0.24 | 0.25 | 0.26 | 0.28 | 0.30 | 0.32 | 0.34 | 0.36 |
| | 1.25 | 0.21 | 0.21 | 0.22 | 0.23 | 0.24 | 0.26 | 0.27 | 0.29 | 0.31 |
| | 1.5 | 0.18 | 0.19 | 0.19 | 0.20 | 0.22 | 0.23 | 0.24 | 0.26 | 0.28 |
| | 1.75 | 0.17 | 0.17 | 0.18 | 0.19 | 0.20 | 0.21 | 0.22 | 0.24 | 0.26 |
| | 2 | 0.16 | 0.16 | 0.17 | 0.17 | 0.18 | 0.20 | 0.21 | 0.22 | 0.24 |

Table 7. Time budget for drone collection using more optimized flight settings and better data transfer technology. Figures are calculated from advertised capabilities of the used drone system.

| **Optimized Collection (Adjusted to min/Km)** | | |
|---|---|---|
| | Time (Min) | Time (Hr) |
| Set Up | 15 | 0.25 |
| Calibration | 2 | 0.03 |
| Flight | 10 | 0.17 |
| Moving Pics to Computer | 10 | 0.17 |

| **Pilot Total (Optimized, Hr/Km):** | 0.62 |
|---|---|

Table 8. Proportionate comparison of the cost per kilometer, calculated as traditional / drone cost for the optimized drone flight times and original traditional inspection overhead. Proportionate comparisons are shown across variances in inspector walking speed and GIS processing time reductions achieved through more efficient computing. Traditional inspections are applying a 25% overhead. Drone flight times have been optimized in this scenario Results closer to 1 denote costs closer in similarity. Cells containing values with less than 10% difference, or which favor drone inspections are highlighted in green.

| | | $/Km Proportional Cost Comparison | | | | | | | | |
|---|---|---|---|---|---|---|---|---|---|---|
| | | Drone Processing Efficiency Increase with Flight Optimization | | | | | | | | |
| | | 0% | 5% | 10% | 20% | 30% | 40% | 50% | 60% | 70% |
| Inspector Speed (mph) 25% Overhead | 0.25 | 0.78 | 0.81 | 0.83 | 0.88 | 0.94 | 1.00 | 1.08 | 1.16 | 1.26 |
| | 0.5 | 0.43 | 0.45 | 0.46 | 0.49 | 0.52 | 0.55 | 0.60 | 0.64 | 0.70 |
| | 0.75 | 0.32 | 0.33 | 0.34 | 0.36 | 0.38 | 0.41 | 0.44 | 0.47 | 0.51 |
| | 1 | 0.26 | 0.27 | 0.27 | 0.29 | 0.31 | 0.33 | 0.36 | 0.38 | 0.42 |
| | 1.25 | 0.22 | 0.23 | 0.24 | 0.25 | 0.27 | 0.29 | 0.31 | 0.33 | 0.36 |
| | 1.5 | 0.20 | 0.21 | 0.21 | 0.23 | 0.24 | 0.26 | 0.28 | 0.30 | 0.32 |
| | 1.75 | 0.18 | 0.19 | 0.20 | 0.21 | 0.22 | 0.24 | 0.25 | 0.27 | 0.30 |
| | 2 | 0.17 | 0.18 | 0.18 | 0.19 | 0.21 | 0.22 | 0.24 | 0.26 | 0.28 |

Table 9. Proportionate comparison of the cost per kilometer, calculated as traditional / drone cost for the optimized drone flight times and the increased traditional inspection overhead. Proportionate comparisons are shown across variances in inspector walking speed and GIS processing time reductions achieved through more efficient computing. Traditional inspections are applying a 40% overhead. Drone flight times have been optimized in this scenario Results closer to 1 denote costs closer in similarity. Cells containing values with less than 10% difference, or which favor drone inspections are highlighted in green.

| | | $/Km Proportional Cost Comparison | | | | | | | | |
|---|---|---|---|---|---|---|---|---|---|---|
| | | Drone Processing Efficiency Increase with Flight Optimization | | | | | | | | |
| | | 0% | 5% | 10% | 20% | 30% | 40% | 50% | 60% | 70% |
| Inspector Speed (mph) 40% Overhead | 0.25 | 0.88 | 0.90 | 0.93 | 0.98 | 1.05 | 1.12 | 1.20 | 1.30 | 1.41 |
| | 0.5 | 0.48 | 0.50 | 0.51 | 0.54 | 0.58 | 0.62 | 0.66 | 0.72 | 0.78 |
| | 0.75 | 0.35 | 0.36 | 0.37 | 0.40 | 0.42 | 0.45 | 0.49 | 0.52 | 0.57 |
| | 1 | 0.29 | 0.30 | 0.31 | 0.32 | 0.35 | 0.37 | 0.40 | 0.43 | 0.47 |
| | 1.25 | 0.25 | 0.26 | 0.26 | 0.28 | 0.30 | 0.32 | 0.34 | 0.37 | 0.40 |
| | 1.5 | 0.22 | 0.23 | 0.24 | 0.25 | 0.27 | 0.29 | 0.31 | 0.33 | 0.36 |
| | 1.75 | 0.21 | 0.21 | 0.22 | 0.23 | 0.24 | 0.26 | 0.28 | 0.30 | 0.33 |
| | 2 | 0.19 | 0.20 | 0.20 | 0.21 | 0.23 | 0.24 | 0.26 | 0.28 | 0.31 |

## Appendix A.

Each image captures a different sheet from the Excel model developed to calculate and output cost comparison analysis for the drone and traditional inspections.

| | | | | | | | | | | | | | |
|---|---|---|---|---|---|---|---|---|---|---|---|---|---|
| Traditional Inspection | | | | | | | | | | | | | |
| | Equipment Costs | | | | | | | | | | | | |
| | | Item/License | Cost ($) | Qty | Replacement Period (yrs) | $/yr | $/Km | | | | Traditional | UAV | |
| | | iPad | 599 | 1 | 1 | $ 599.00 | $ 2.27 | | | Technology | 6% | 21% | |
| | | Apple iCare | 149 | 1 | 2 | $ 74.50 | $ 0.28 | | | Labor | 94% | 79% | |
| | | | | | | | $ 2.55 | 6% | | | | | |
| | Manpower Costs | | | | | | | | | | | | |
| | | Position | Hourly Rate | Hourly Rate + 25% | | Hrs/Km | $/Km | | | | | | |
| | | Pipeline Inspector* | 20 | 25 | | 1.742742 | $ 43.57 | 94% | | | | | |
| | | | | | | | | | | | | | |
| | | | | | | Traditional Total $/Km: | $ 46.12 | | | | | | |
| Drone Inspection | | | | | | | | | | | | | |
| | Equipment Costs | | | | | | | | | | | | |
| | | Item/License | Cost ($) | Qty | Replacement Period (yrs) | $/yr | $/Km | | | | | | |
| | | DJI M200 v2** | 6000 | 1 | 13.25 | $ 452.83 | $ 1.71 | 4% | | | | | |
| | | Drone Insurance*** | 728.06 | 1 | 1 | $ 728.06 | $ 2.75 | 7% | | | | | |
| | | M200 Battery | 480 | 2 | 1.7 | $ 564.71 | $ 2.14 | 5% | | | 24% | | |
| | | Sentera 6x Multispectral Sensor | 13550 | 1 | 13.25 | $ 1,022.64 | $ 3.87 | 9% | | | | | |
| | | iPad | 599 | 1 | 1 | $ 599.00 | $ 2.27 | 6% | | | | | |
| | | Apple iCare | 149 | 1 | 2 | $ 74.50 | $ 0.28 | 1% | | | | | |
| | | Pix4d Mapper | 3600 | 1 | 1 | $ 3,600.00 | $ 13.61 | 33% | | | | | |
| | | Esri ArcGIS Pro License | 3800 | 1 | 1 | $ 3,800.00 | $ 14.37 | 35% | | | | | |
| | | | | | | | $ 41.00 | | | | | | |
| | Manpower Costs | | | | | | | | | | | | |
| | | Position | Hourly Rate | Hourly Rate + 25% | | Hrs/Km | $/Km | | | | | | |
| | | Pilot | 20 | 25 | | 1.283333333 | $ 32.08 | 21% | | | | | |
| | | GIS Analyst | 40 | 50 | | 2.425 | $ 121.25 | 79% | | | | | |
| | | | | | | | $ 153.33 | | | | | | |
| | | | | | | Drone Total $/Km | $ 194.34 | | | | | | |
| | | | | | | | | | | | | | |
| * -Where applicable, ground inspector travel speed at 1 mi/ Hr as reported by industry advisors, and 25% overhead as reported by SBA.gov | | | | | | | | | | | | | |
| ** - Drone used is no longer being produced. Price used is listed price for a new old-stock model | | | | | | | | | | | | | |
| *** - Estimate retrieved from: https://www.droneblog.com/how-much-does-drone-insurance-cost/ | | | | | | | | | | | | | |

| Inspector Speed Mph | Cost (25% Overh | Cost (40% Overhead |
|---|---|---|
| 0.25 | $ 139.32 | $ 155.73 |
| 0.5 | $ 77.18 | $ 86.14 |
| 0.75 | $ 56.47 | $ 62.94 |
| 1 | $ 46.12 | $ 51.34 |
| 1.25 | $ 39.90 | $ 44.38 |
| 1.5 | $ 35.76 | $ 39.74 |
| 1.75 | $ 32.80 | $ 36.43 |
| 2 | $ 30.58 | $ 33.95 |

| Processing Increase | Current Flight | Optimized Flight Setup |
|---|---|---|
| 0 | $ 194.34 | $ 177.67 |
| 10 | $ 184.71 | $ 168.04 |
| 20 | $ 175.09 | $ 158.42 |
| 30 | $ 165.46 | $ 148.79 |
| 40 | $ 155.84 | $ 139.17 |
| 50 | $ 146.21 | $ 129.54 |
| 60 | $ 136.59 | $ 119.92 |
| 70 | $ 126.96 | $ 110.29 |

0.754269

| | Efficiency I | Walking Speed |
|---|---|---|
| Base Case | 0% | 1 |

| | Efficiency Increase | | | | | | | | |
|---|---|---|---|---|---|---|---|---|---|
| Walking Sp | 24% | 5% | 10% | 20% | 30% | 40% | 50% | 60% | 70% |
| 0.25 | 3.737638 | 1.913004 | 1.000687 | 0.696582 | 0.544528922 | 0.453297229 | 0.3924761 | 0.349032437 | |
| 0.5 | 4.352758 | 2.227836 | 1.165375 | 0.811221 | 0.634144551 | 0.527898439 | 0.457067697 | 0.40647431 | |
| 0.75 | 5.21023 | 2.666709 | 1.394948 | 0.971028 | 0.759067836 | 0.631891774 | 0.547107733 | 0.486547703 | |
| 1 | 6.488415 | 3.320912 | 1.73716 | 1.209243 | 0.945284033 | 0.786908859 | 0.681325409 | 0.60590866 | |
| 1.25 | 8.597596 | 4.400436 | 2.301856 | 1.60233 | 1.252566382 | 1.042708379 | 0.902803044 | 0.802870662 | |
| 1.5 | 12.73848 | 6.51983 | 3.410505 | 2.374064 | 1.855843066 | 1.544910628 | 1.337622337 | 1.189559271 | |
| 1.75 | 24.57422 | 12.57762 | 6.579319 | 4.579886 | 3.580168674 | 2.980338552 | 2.580451803 | 2.294818412 | |
| 2 | 346.7669 | 177.4828 | 92.84079 | 64.62677 | 50.51976594 | 42.05556211 | 36.41275956 | 32.38218631 | |

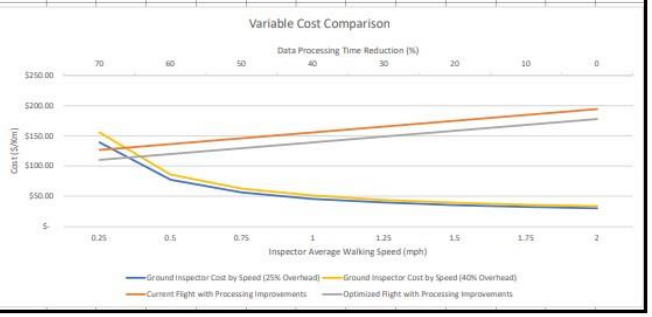

| Large Costs | | | | | | | |
|---|---|---|---|---|---|---|---|
| | Gear | Cost | Years | | | | |
| | Boots | 150 | 1 | | | | |
| | iPad | 599 | 1 | | | | |
| | Apple Care | 149 | 2 | | | | |
| | Adobe Lice | 200 | 1 | | | | |
| | Worker Ins | UNK | | | | | |
| | | | | | | 2.5 miles per job | |
| Individual Inspection Cost | | | | | | | |
| | Position | Rate/Hr | Rate + 25% overhead | | | | |
| | Inspector | 20 | 25 | | | | |
| | Supervisor | 65 | 81.25 | | | | |

| All Times are in Hours or Days as appropriate, Self reporting is 1 mph | | | | | | | | | | | | | | | | |
|---|---|---|---|---|---|---|---|---|---|---|---|---|---|---|---|---|
| Task | Speed (mph) | Hrs/site mi | Hrs/site Km | Miles/Site | Km/Site | Sites/Day | Inspection Km/ | Sites/Wk | Insp Km/Week | Inspection Hours/Wk | | Fixed | Hrs/Site | Hrs/Day | Hrs/Wk | Hrs/Km |
| Pipeline | 1 | 2 | 1.242742 | 2.5 | 4.023361245 | 2.5 | 20.11680622 | 12.5 | 100.5840311 | 62.5 | | Report | 0.5 | 1.5 | 7.5 | 0.07456452 |
| | | | | | | | | | | | | | | | | |
| | | | | | | | | | | | | | | | | |
| | | | | | | | | | | | | | | | | |
| | | | | | | | | | | | | | | | | |
| | | Inspection + Report For 1 Site (Hr/Km) | 1.742742 | | | | | | | | | | | | | |
| | | $/Km | 43.56855 | | | | | | | | | | | | | |
| | | | | | | | | | | | | | | | | |
| | | | | | | | | | | | | | | | | |
| Average Inspector Speed (mph) | | | | | | | | | | | | | | | | |
| Average Site Length in Miles | | | | | | | | | | | | | | | | |
| Average Sites Per Day | | | | | | | | | | | | | | | | |

| Field Technician/Flight | | | | | Master Set | | | | Time Min | Time Hr |
|---|---|---|---|---|---|---|---|---|---|---|
| | Collection (per Km) | Time Min | Time Hr | | Collection (per Km) | Time Min | Time Hr | | 15 | 0.25 |
| | Set Up | 30 | 0.5 | | Set Up | 30 | 0.5 | | 2 | 0.033333 |
| | Calibration | 2 | 0.033333333 | | Calibration | 2 | 0.033333333 | | 10 | 0.166667 |
| | Flight | 20 | 0.333333333 | | Flight | 20 | 0.333333333 | | 10 | 0.166667 |
| | Moving Pics to Computer | 25 | 0.416666667 | | Moving Pics to Computer | 25 | 0.416666667 | | 37 | 0.616667 |
| | Total | 77 | 1.283333333 | | Total | 77 | 1.283333333 | | 37 | 0.616667 |
| Pilot Total-> | Per KM Total | 77 | 1.283333333 | | Per KM Total | 77 | 1.283333333 | | | |
| GIS Analysit | | | | | | | | | | |
| | Pix 4D (per KM) | Time Min | Time Hr | | Pix 4D (per KM) | Time Min | Time Hr | | | |
| | Align | 45 | 0.75 | | Align | 45 | 0.75 | | | |
| | Set GCP | 30 | 0.5 | | Set GCP | 30 | 0.5 | | | |
| | Products | 20 | 0.333333333 | | Products | 20 | 0.333333333 | | | |
| | Total | 95 | 1.583333333 | | Total | 95 | 1.583333333 | | | |
| | Per KM Total | 95 | 1.583333333 | | Per KM Total | 95 | 1.583333333 | | | |
| | | | | | | | | | | |
| | Arc (Whole Site) | Time Min | Time Hr | | Arc (Whole Site) | Time Min | Time Hr | | | |
| | Load | 15 | 0.25 | | Load | 15 | 0.25 | | | |
| | Mosaic | 2 | 0.033333333 | | Mosaic | 2 | 0.033333333 | | | |
| | Calculate NDVI | 1 | 0.016666667 | | Calculate NDVI | 1 | 0.016666667 | | | |
| | Clip | 1 | 0.016666667 | | Clip | 1 | 0.016666667 | | | |
| | Check Training Features | 20 | 0.333333333 | | Check Training Features | 20 | 0.333333333 | | | |
| | Train SVM | 1 | 0.016666667 | | Train SVM | 1 | 0.016666667 | | | |
| | Reclassify | 1 | 0.016666667 | | Reclassify | 1 | 0.016666667 | | | |
| | Total | 41 | 0.683333333 | | Total | 41 | 0.683333333 | | | |
| | Per KM Total | 20.5 | 0.341666667 | | Per KM Total | 20.5 | 0.341666667 | | | |
| | | | | | | | | | | |
| | Efficiency Increase: | 0% | 1.925 | | | | | | | |
| Report Creator | | | | | | | | | | |
| | Report Step | Time Min | Time Hr | | Report Step | Time Min | Time Hr | | | |
| | Analysis (Review) | 30 | 0.5 | | Analysis (Review) | 30 | 0.5 | | | |
| | Report | 30 | 0.5 | | Report | 30 | 0.5 | | | |
| | Total | 60 | 1 | | Total | 60 | 1 | | | |
| | Per KM Total | 30 | 0.5 | | Per KM Total | 30 | 0.5 | | | |
| | | | | | | | | | | |
| | GIS Analyst total-> | | 2.425 | | | | | | | |
| | | | | | | | | | | |
| | | | | | | | | | | |
| Processing Optimization | | | | | | | | | | |

| Multispectral DJI | | | | | | | | | | | | | | | | |
|---|---|---|---|---|---|---|---|---|---|---|---|---|---|---|---|---|
| Gear | Cost | Quantity Needed | Time Count | Time Type | | | | Fixed Costs | | | | | | | | |
| DJI P4 Multispectral | 9100 | 1 | 5 | Year | | | | | | | | | | | | |
| DJI Phantom 4 Battery | 185 | 3 | 1 | Year | Buy Phantom 4 Series Intelligent Flight Battery - DJI Store | | | Gear | Cost | Quantity Needed | Time Count | Time Type | | | | |
| | | | | | | | | iPad | 599 | 1 | 1 | Year | AppleCare Products - iPad - Apple | | | |
| | | | | | | | | Apple Care | 149 | 1 | 2 | Year | AppleCare Products - iPad - Apple | | | |
| | | | | | | | | Pix4d Mapper | 3600 | 1 | 1 | N/A | Pricing plans for PIX4Dmapper photogrammetry software \| Pix4D | | | |
| | | | | | | | | Drone Insurance | 728.06 | 1 | 1 | Year | How Much Does Drone Insurance Cost? – Droneblog | | | |
| Insurance? | | | | | | | | Adobe License (Approximate) | 200 | 1 | 1 | Year | | | | |
| | | | | | | | | Arc | 3800 | 1 | 1 | | | | | |
| | | | | | | | | | | | | | | | | |
| RGB DJI | | | | | | | | | | | | | | | | |
| Gear | Cost | Quantity Needed | Time Count | Time Type | | | | | | | | | | | | |
| DJI Phantom 4 Pro V.2 | 1600 | 1 | 5 | Year | Phantom 4 Pro V2.0 - Professional Aerial Filmmaking Made Easy (dji.com) | | | | | | | | | | | |
| DJI Phantom 4 Battery | 185 | 3 | 1 | Year | Buy Phantom 4 Series Intelligent Flight Battery - DJI Store | | | | | | | | | | | |
| | | | | | | | | | | | | | | | | |
| | | | | | | | | | | | | | | | | |
| | | | | | | | | Pay Rates | $/Hr | $/Hr + 25% | | | | | | |
| | | | | | | | | Field Collection | 20 | 25 | | | | | | |
| | | | | | | | | Gis Specialist | 40 | 50 | | | | | | |
| | | | | | | | | | | | | | | | | |
| | | | | | | | | | | | | | | | | |
| | | | | | | | | | | | | | | | | |
| | | | | | | | | | | | | | | | | |
| Sentera Long Range | | | | | | | | | | | | | | | | |
| Gear | Cost | Quantity Needed | Time Count | Time Type | | | | | | | | | | | | |
| Sentera Double 4K PHX Ag+ | 11000 | 1 | 5 | Year | Double 4K PHX (sentera.shop) | | | | | | | | | | | |
| Sentera PHX Batteries | 400 | 3 | 1 | Year | PHX Battery (sentera.shop) | | | | | | | | | | | |
| | | | | | | | | | | | | | | | | |
| | | | | | | | | | | | | | | | | |
| | | | Years | | | | | | Item Life Calculations | | | | | | | |
| M200 | 6000 | 1 | 26.5 | | | | | | | Drone Life | Flight Hours | Time per flight | Number of Flights | | Flights/Year | Years of Use |
| M200 Batt | 480 | 2 | 1.7 | | | <-200 Cycles | | | | DJI M200 | 1000 | 0.333333333 | | 3000 | 113 | 26.5486726 |
| Sentera 6x | 13550 | 1 | 26.5 | | | One Time Purchase | | | | DJI M200 Batteries | | | | 200 | 113 | 1.7699115 |

| Alternative | | | | | | | | | Miles/Branch | KM/Branch | | | | |
|---|---|---|---|---|---|---|---|---|---|---|---|---|---|---|
| | | | | | | | | | 2.5 | 4.023361245 | | | | |
| | | | | | | | | | | | | | | |
| | Speed | M/s | Km/Hr | mph | Fligth Time (min) | Flight time (hrs) | Km/Flight | Linear Km W/ Return | Branch/Flight | % Change | | | | |
| | DJI Phantom 4v2 | 16.11111111 | 58 | | 20 | 0.333333333 | 19.33333333 | 9.666666667 | 2.402634533 | -0.052287582 | | | | |
| Current -> | DJI M200 v2 | 17 | 61.2 | | 20 | 0.333333333 | 20.4 | 10.2 | 2.53519368 | | | | | |
| | Sentera PHX | 13.41116667 | 48.2802 | 30 | 40 | 0.666666667 | 32.1868 | 16.0934 | 3.999988821 | 0.577784314 | | <- Over 1 day worth of inspections | | |
| | | 6 | 21.6 | 30 | 20 | 0.333333333 | 7.2 | 3.6 | 0.89477424 | | | | | |
| | | | | | | | | | | | | | | |
| Field Technician/Flight | | | | | | | | | | | | | | |
| | Collection ( | Time Min | Time Hr | | | | | | | | | | | |
| | Set Up | 30 | 0.5 | | | | | | | | | | | |
| | Calibration | 2 | 0.033333333 | | | | | | | | | | | |
| | Flight | 20 | 0.333333333 | | | | | | | | | | | |
| | Moving Pics to Computer | 25 | 0.416666667 | | | | | | | | | | | |
| | Total | 77 | 1.283333333 | | | | | | | | | | | |
| | Per KM Total | 77 | 1.283333333 | | | | | | | | | | | |
| GIS Analysit | | | | | | | | | | | | | | |
| | Pix 4D | Time Min Per Km | Time Hr Per Km | New Hr (whole) | | | | | | | | | | |
| | Align | 45 | 0.75 | 12.07005 | | | | | | | | | | |
| | Set GCP | 30 | 0.5 | 8.0467 | | | | | | | | | | |
| | Products | 20 | 0.333333333 | 5.364467 | | | | | | | | | | |
| | Total | 95 | 1.583333333 | 25.48122 | | | | | | | | | | |
| | Per KM Total | 95 | 1.583333333 | 1.583333 | | | | | | | | | | |
| | | | | | | | | | | | | | | |
| | Arc (Whole Site) | Time Min | Time Hr | | | | | | | | | | | |
| | Load | 15 | 0.25 | | | | | | | | | | | |
| | Mosaic | 2 | 0.033333333 | | | | | | | | | | | |
| | Calculate NDVI | 1 | 0.016666667 | | | | | | | | | | | |
| | Clip | 1 | 0.016666667 | | | | | | | | | | | |
| | Check Training Features | 20 | 0.333333333 | | | | | | | | | | | |
| | Train SVM | 1 | 0.016666667 | | | | | | | | | | | |
| | Reclassify | 1 | 0.016666667 | | | | | | | | | | | |
| | Total | 41 | 0.683333333 | | | | | | | | | | | |
| | Per KM Total | 20.5 | 0.341666667 | | | | | | | | | | | |
| | | | | | | | | | | | | | | |
| Report Creator | | | | | | | | | | | | | | |
| | Report Step | Time Min | Time Hr | | | | | | | | | | | |
| | Analysis (Review) | 30 | 0.5 | | | | | | | | | | | |
| | Report | 30 | 0.5 | | | | | | | | | | | |
| | Total | 60 | 1 | | | | | | | | | | | |
| | Per KM Total | 30 | 0.5 | | | | | | | | | | | |

| Branch | Approx Length (km) | |
|---|---|---|
| S | 1180 | |
| N | 1160 | |
| | | |
| | | |
| Total (km) | 2.34 | |
| Totla (mi) | 1.454008 | |

| | | | | | | | | | | | |
|---|---|---|---|---|---|---|---|---|---|---|---|
| | Inspection | Count | | | Data Search \| National Centers for Environmental Information (NCEI) (noaa.gov) | | | | | | |
| | Weekly | 52 | | | 2021 | 2020 | 2019 | | | | |
| | Rain | 60.66667 | | | 50 | 62 | 70 | | 182 | | |
| | | | | | | | | | | | |
| | Total Inspe | 113 | | | | | | | | | |
| | Total Km/Y | 264.42 | | | | | | | | | |

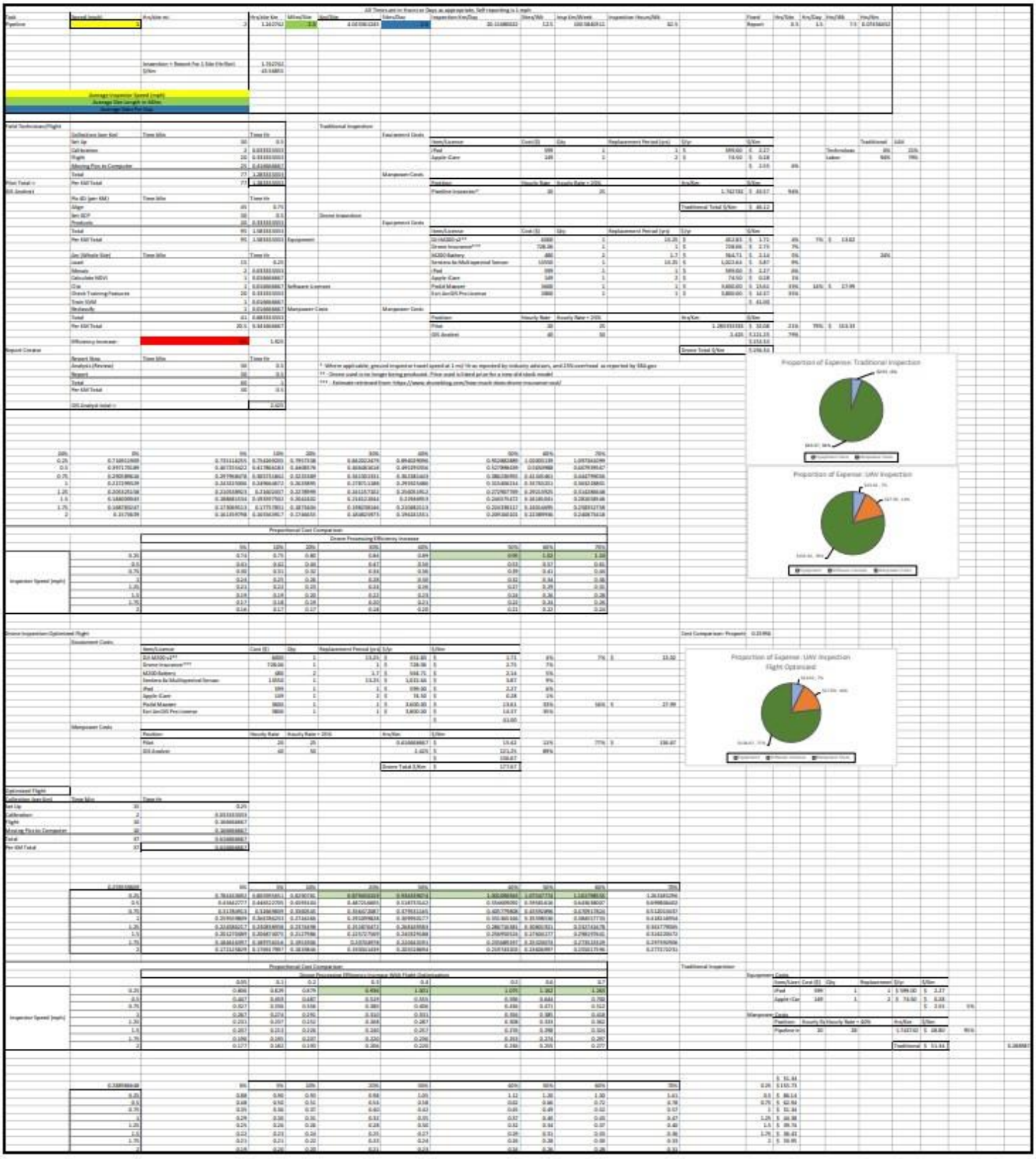

Traditional Inspection

Equipment Costs

| Item/License | Cost ($) | Qty | Replacement Period (yrs) | $/yr | $/km | % of Method Total |
|---|---|---|---|---|---|---|
| iPad | $ 599.00 | 1 | 1 | $ 599.00 | $ 2.27 | 5% |
| Apple iCare | $ 149.00 | 1 | 2 | $ 74.50 | $ 0.28 | 1% |
| | | | Equipment Cost Subtotal ($/km) | | $ 2.55 | 6% |

Manpower Costs

| Position | Rate ($/hr) | Rate + 25% ($/hr) | Hrs/km | $/km | |
|---|---|---|---|---|---|
| Pipeline Inspector* | $ 20.00 | $ 25.00 | 1.74 | $ 43.57 | 94% |
| | | Traditional Inspection Cost Total ($/km): | | $ 46.12 | |

Drone Inspection

Equipment Costs

| Item/License | Cost ($) | Qty | Replacement Period (yrs) | $/yr | $/km | % of Method Total |
|---|---|---|---|---|---|---|
| DJI M350 w/** | $ 6,000.00 | 1 | 13.25 | $ 452.83 | $ 1.71 | 1% |
| Drone Insurance*** | $ 728.06 | 1 | 1 | $ 728.06 | $ 2.75 | 1% |
| M300 Battery | $ 480.00 | 2 | 1.7 | $ 564.71 | $ 2.14 | 1% |
| Sentera 6x Multispectral Sensor | $ 13,550.00 | 1 | 13.25 | $ 1,022.64 | $ 3.87 | 2% |
| iPad | $ 599.00 | 1 | 1 | $ 599.00 | $ 2.27 | 1% |
| Apple iCare | $ 149.00 | 1 | 2 | $ 74.50 | $ 0.28 | 0% |
| PIX4DMapper | $ 3,600.00 | 1 | 1 | $ 3,600.00 | $ 13.61 | 7% |
| ArcGIS Pro License | $ 3,800.00 | 1 | 1 | $ 3,800.00 | $ 14.37 | 7% |
| | | | Equipment Cost Subtotal ($/km) | | $ 41.00 | 21% |

Manpower Costs

| Position | Hourly Rate | Hourly Rate + 25% | Hrs/km | $/km | |
|---|---|---|---|---|---|
| Pilot | $ 20.00 | $ 25.00 | 1.28 | $ 32.08 | 17% |
| GIS Analyst | $ 40.00 | $ 50.00 | 2.43 | $ 121.25 | 62% |
| | | Manpower Cost Subtotal ($/km) | | $ 153.33 | 79% |
| | | Drone Inspection Cost Total ($/km): | | $ 194.34 | |

* - Where applicable, ground inspector travel speed at 1 mi/ Hr as reported by industry advisors, and 25% overhead as reported by SBA.gov

** - Drone used is no longer being produced. Price used is listed price for a new old-stock model

*** - 1st million retrieved from: https://www.droneblog.com/how-much-does-drone-insurance-cost/

Collection (Adjusted to min/km)

| | Time (Min) | Time (Hr) |
|---|---|---|
| Set Up | 30 | 0.50 |
| Calibration | 2 | 0.03 |
| Flight | 20 | 0.33 |
| Moving Pics to Computer | 25 | 0.42 |
| Pilot Total (Hr/km): | | 1.28 |

Processing (Adjusted to min/km)

| | Time (Min) | Time (Hr) |
|---|---|---|
| Align | 45 | 0.75 |
| Set GCP | 30 | 0.50 |
| Products | 20 | 0.33 |
| Processing Subtotal (Hr/km): | | 1.58 |

Modeling

| | Time (Min) | Time (Hr) |
|---|---|---|
| Load | 15 | 0.25 |
| Mosaic | 2 | 0.03 |
| Calculate NDVI | 1 | 0.02 |
| Clip | 1 | 0.02 |
| Check Training Features | 20 | 0.33 |
| Train SVM | 1 | 0.02 |
| Reclassify | 1 | 0.02 |
| Total | 41 | 0.68 |
| Modeling Subtotal (Hr/km): | | 0.34 |

Analysis and Report Creation

| | Time (Min) | Time (Hr) |
|---|---|---|
| Analysis (Review) | 30 | 0.50 |
| Report | 30 | 0.50 |
| Total | 60 | 1.00 |
| Analysis and Report Subtotal (Hr/km): | | 0.50 |
| GIS Analyst total (Hr/km): | | 2.43 |

Optimized Collection (Adjusted to min/km)

| | Time (Min) | Time (Hr) |
|---|---|---|
| Set Up | 15 | 0.25 |
| Calibration | 2 | 0.03 |
| Flight | 10 | 0.17 |
| Moving Pics to Computer | 10 | 0.17 |
| Pilot Total (Optimized, Hr/km): | | 0.62 |

$/Km Proportional Cost Comparison

Drone Processing Efficiency Increase

| Inspector Speed (mph) 25% Overhead | 0% | 5% | 10% | 20% | 30% | 40% | 50% | 60% | 70% |
|---|---|---|---|---|---|---|---|---|---|
| 0.25 | 0.72 | 0.76 | 0.75 | 0.80 | 0.84 | 0.89 | 0.95 | 1.02 | 1.10 |
| 0.5 | 0.40 | 0.41 | 0.42 | 0.44 | 0.47 | 0.50 | 0.53 | 0.57 | 0.61 |
| 0.75 | 0.29 | 0.30 | 0.31 | 0.32 | 0.34 | 0.36 | 0.39 | 0.41 | 0.44 |
| 1 | 0.24 | 0.24 | 0.25 | 0.26 | 0.28 | 0.30 | 0.32 | 0.34 | 0.36 |
| 1.25 | 0.21 | 0.21 | 0.22 | 0.23 | 0.24 | 0.26 | 0.27 | 0.29 | 0.31 |
| 1.5 | 0.18 | 0.19 | 0.19 | 0.20 | 0.22 | 0.23 | 0.24 | 0.26 | 0.28 |
| 1.75 | 0.17 | 0.17 | 0.18 | 0.19 | 0.20 | 0.21 | 0.22 | 0.24 | 0.26 |
| 2 | 0.16 | 0.16 | 0.17 | 0.17 | 0.18 | 0.20 | 0.21 | 0.22 | 0.24 |

$/Km Proportional Cost Comparison

Drone Processing Efficiency Increase With Flight Optimization

| Inspector Speed (mph) 25% Overhead | 0% | 5% | 10% | 20% | 30% | 40% | 50% | 60% | 70% |
|---|---|---|---|---|---|---|---|---|---|
| 0.25 | 0.78 | 0.81 | 0.83 | 0.88 | 0.94 | 1.00 | 1.08 | 1.16 | 1.26 |
| 0.5 | 0.43 | 0.45 | 0.46 | 0.49 | 0.52 | 0.55 | 0.60 | 0.64 | 0.70 |
| 0.75 | 0.32 | 0.33 | 0.34 | 0.36 | 0.38 | 0.41 | 0.44 | 0.47 | 0.51 |
| 1 | 0.26 | 0.27 | 0.27 | 0.29 | 0.31 | 0.33 | 0.36 | 0.38 | 0.42 |
| 1.25 | 0.22 | 0.23 | 0.24 | 0.25 | 0.27 | 0.29 | 0.31 | 0.33 | 0.36 |
| 1.5 | 0.20 | 0.21 | 0.21 | 0.23 | 0.24 | 0.26 | 0.28 | 0.30 | 0.32 |
| 1.75 | 0.18 | 0.19 | 0.20 | 0.21 | 0.22 | 0.24 | 0.25 | 0.27 | 0.30 |
| 2 | 0.17 | 0.18 | 0.18 | 0.19 | 0.21 | 0.22 | 0.24 | 0.26 | 0.28 |

$/Km Proportional Cost Comparison

Drone Processing Efficiency Increase With Flight Optimization

| Inspector Speed (mph) 40% Overhead | 0% | 5% | 10% | 20% | 30% | 40% | 50% | 60% | 70% |
|---|---|---|---|---|---|---|---|---|---|
| 0.25 | 0.88 | 0.90 | 0.93 | 0.98 | 1.05 | 1.13 | 1.20 | 1.30 | 1.40 |
| 0.5 | 0.48 | 0.50 | 0.51 | 0.54 | 0.58 | 0.62 | 0.66 | 0.72 | 0.78 |
| 0.75 | 0.35 | 0.36 | 0.37 | 0.40 | 0.42 | 0.45 | 0.49 | 0.52 | 0.57 |
| 1 | 0.29 | 0.30 | 0.31 | 0.32 | 0.35 | 0.37 | 0.40 | 0.43 | 0.47 |
| 1.25 | 0.25 | 0.26 | 0.26 | 0.28 | 0.30 | 0.32 | 0.34 | 0.37 | 0.40 |
| 1.5 | 0.22 | 0.23 | 0.24 | 0.25 | 0.27 | 0.29 | 0.31 | 0.33 | 0.36 |
| 1.75 | 0.21 | 0.21 | 0.22 | 0.23 | 0.24 | 0.26 | 0.28 | 0.30 | 0.33 |
| 2 | 0.19 | 0.20 | 0.20 | 0.21 | 0.23 | 0.24 | 0.26 | 0.28 | 0.31 |